

## 中国蛇绿岩型铬铁矿的研究进展及思考

胡振兴<sup>1\*</sup>, 牛耀龄<sup>2,3,4\*</sup>, 刘益<sup>4</sup>, 张国瑞<sup>1</sup>, 孙文礼<sup>1</sup>, 马玉鑫<sup>1</sup>

1. 兰州大学 地质科学与矿产资源学院, 兰州 730000; 2. Department of Earth Sciences, Durham University, Durham DH1 3LE, UK; 3. 中国科学院 海洋研究所, 青岛 266071; 4. 中国地质大学 地球科学与资源学院, 北京 100083

**摘要:** 中国广泛分布有不同时期的蛇绿岩。相对于全球一些大型蛇绿岩铬铁矿床(如Kempirsai, Bulquiza, Guleman等),我国同期蛇绿岩中赋存的铬铁矿床规模都较小(如萨尔托海,东巧,罗布莎等)。近年来的研究认识到绝大多数成矿的蛇绿岩都形成于俯冲带上覆岩石圈。熔-岩反应是目前用来解释豆荚状铬铁矿成因的流行假说,但仍然不能解释铬元素的有效富集过程——即铬铁矿矿床的形成过程。高铬含量是岛弧玄武岩原始岩浆的特征,但与成矿要求的铬含量相差甚远;岛弧原始玄武岩岩浆结晶出富铬尖晶石,有利于成矿,但这个岩浆演化和相平衡过程仍然难以造就具有工业意义的矿体、矿床。那么存在形成富铬熔体的机制吗?又如何运移这些富铬熔体并集中结晶成矿?这些仍然是豆荚状铬铁矿成因的关键问题,有待于进一步思考研究。

**关键词:** 蛇绿岩; 豆荚状铬铁矿; 熔-岩反应; 水; 铬尖晶石

中图分类号: P618.3

文献标识码: A

文章编号: 1006-7493(2014)01-0009-19

## Petrogenesis of Ophiolite-type Chromite Deposits in China and Some New Perspectives

HU Zhenxing<sup>1\*</sup>, NIU Yaoling<sup>2,3,4\*</sup>, LIU Yi<sup>4</sup>, ZHANG Guorui<sup>1</sup>, SUN Wenli<sup>1</sup>, MA Yuxin<sup>1</sup>

1. School of Earth Sciences, Lanzhou University, Lanzhou 730000, China; 2. Department of Earth Sciences, Durham University, Durham DH1 3LE, UK; 3. Institute of Oceanology, Chinese Academy of Sciences, Qingdao 266071, China; 4. China University of Geosciences, Beijing 10083, China

**Abstract:** Ophiolites of varying ages are widespread in China, some of which contain chromite deposits of industrial value. However, compared with some of the world's large ophiolite chromite deposits (e.g., Kempirsai, Bulquiza, Guleman), the Chinese chromite deposits are small (e.g., Sartohay, Dongqiao, Luobusa). Recent research recognizes that most ophiolites with significant chromite reserves are all formed in a subduction zone environment. Melt-rock interaction is a popular interpretation for the origin of podiform chromite deposits, but the actual mechanism in this model for chromite enrichment remains unclear. It remains the primary task to understand process or processes of chromium enrichment towards the formation of chromite deposits. Is the formation of chromium-rich melts necessary? If so, when, where, how, and under what conditions could this take place? These are additional processes beyond the well-understood aspects of the petrogenesis that need to research towards an effective chromite mineralization model.

**Key words:** China; ophiolites; podiform chromite; melt-rock interaction; water; spinel

**Corresponding author:** NIU Yaoling, Professor; E-mail: yaoling.niu@durham.ac.uk

收稿日期: 2013-10-12; 修回日期: 2013-12-8

基金项目: 中国地质调查局地质调查项目(1212011121092; 1212011220928)

作者简介: 胡振兴, 1989年生, 男, 硕士研究生, 矿物、岩石、矿床学专业; E-mail: huzhx12@lzu.edu.cn

\*通讯作者: 牛耀龄, 1959年生, 博士、教授, 从事岩石学和地球化学教学和研究; E-mail: yaoling.niu@durham.ac.uk

铬铁矿矿床为典型岩浆矿床,分为层型(产于层状超镁铁质-镁铁质侵入体)和蛇绿岩型(产于蛇绿岩中的以豆荚状铬铁矿为特征)两类。层型铬铁矿床(如Bushveld和Stillwater)的形成被认为与大规模的熔体混合有关,即高温富镁铁质初始熔体与相对富铝富硅的低温残留熔体(即经过初始橄榄石和尖晶石共同结晶后的熔体)混合会导致铬尖晶石的持续结晶沉淀,并在重力分异等有利条件下堆晶成矿(Irvine, 1977)。豆荚状铬铁矿产于蛇绿岩套壳幔边界(即岩石学莫霍面)附近的地幔橄榄岩中。越来越多的研究表明地幔橄榄岩部分熔融产生的熔体在迁移过程中会与周围的橄榄岩发生熔-岩反应,豆荚状铬铁矿与这些经历熔-岩反应后更加亏损的方辉橄榄岩,尤其是纯橄岩紧密共生(Zhou and Robinson, 1994; Zhou et al., 1996, 2001a; Uysal et al., 2007; Caran et al., 2010; González-Jiménez et al., 2011)。熔-岩反应常被用来解释豆荚状铬铁矿的成因(Arai and Yurimoto, 1994; Zhou et al., 1994; Zhou and Robinson, 1997; Arai, 1997)。

近些年对罗布莎、Ural等豆荚状铬铁矿床的研究发现它们含有超高压矿物如金刚石、柯石英等,指示豆荚状铬铁矿存在深部源区(至少>150 km)(Robinson et al., 2004; Yang et al., 2007, 2009; Yamamoto et al., 2009)。通过对东巧等地豆荚状铬铁矿的Re-Os同位素研究,史仁灯等认为“古老岩石圈地幔残余的参与有助于铬铁矿的形成”(Shi et al., 2007, 2012a, 2012b)。值得注意和思考的是:与全球同期蛇绿岩铬铁矿床相比,为什么中国豆荚状铬铁矿在矿床规模和铬金属储量上都较小?本文的目的是总结我国蛇绿岩型铬铁矿的基本资料和研究现状,旨在掌握基本资料的基础上厘清我们认识这类铬铁矿成矿的思路,为建立成矿过程模型奠定基础。

## 1 豆荚状铬铁矿的岩石学特征

豆荚状铬铁矿多赋存在蛇绿岩套的地幔橄榄岩(如罗布莎)或地壳超镁铁质堆晶岩(如大道尔吉)中(Paktunc, 1990; Roberts and Neary, 1993)。矿体多以透镜状零散分布,受地幔流动应力及其产生的高温变形作用,矿体长轴方向平

行、似平行或局部穿插围岩(纯橄岩或方辉橄榄岩)面理(Cassard et al., 1981)。

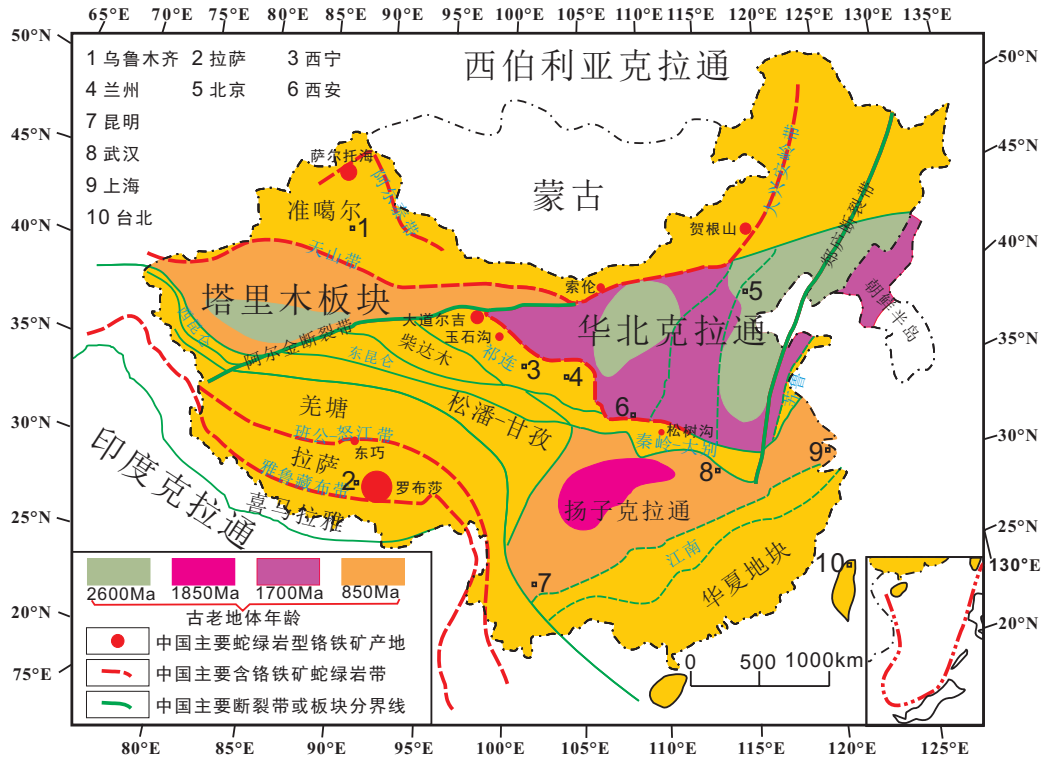
豆荚状铬铁矿矿石根据结晶颗粒大小、聚合形状及密集程度主要分为浸染状,豆荚状,角砾状等结构。与层型铬铁矿相比,豆荚状结构是豆荚状铬铁矿的特有结构,并可随着铬铁矿含量的增加过渡为稀疏浸染状结构、稠密浸染状结构(Robinson et al., 1997)。

豆荚状铬铁矿铬尖晶石常常具有硅酸盐包裹体(韭闪石,金云母等)。这些含水硅酸盐包裹体以熔体状态在铬尖晶石生长过程中被捕获,并与铬尖晶石发生高温反应(Edwards et al., 2000 and therein)。

## 2 中国豆荚状铬铁矿主要产地及全球对比

中国蛇绿岩超基性岩体接近9000个,截至1993年底共发现56个铬矿区(姚培慧, 1996),近年来陆续在休古嘎布、东波、库地等蛇绿岩体新发现铬铁矿矿化点(黄圭成等, 2007; 杨经绥等, 2011; 李军等, 2012)。中国主要豆荚状铬铁矿区分布在典型的造山带蛇绿岩中(图1):如中亚带(新疆萨尔托海,内蒙古贺根山,内蒙古索伦山等),祁连-秦岭带(甘肃大道尔吉,青海玉石沟,陕西松树沟),班公-怒江带(西藏东巧),雅鲁藏布带(西藏罗布莎)(Zhou and Bai, 1992; 鲍佩声等, 1999)。这4个重要的成矿带依次对应着古大洋演化史上4个重要的构造域:古亚洲洋域,原特提斯洋域,中特提斯洋域,新特提斯洋域(Zhang et al., 2008b; Stampfli and Borel, 2002; Metcalfe, 2013)。

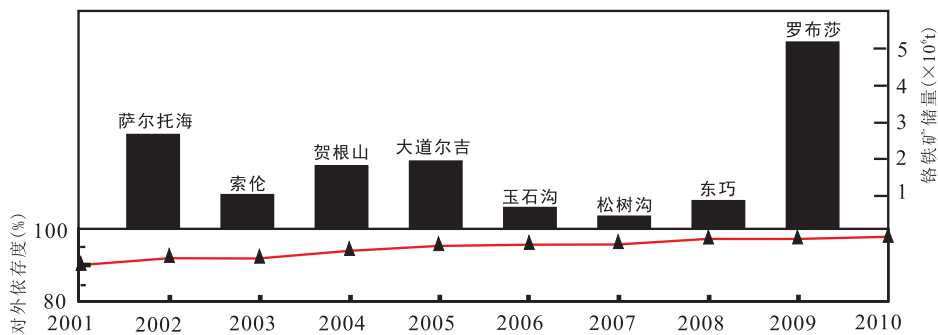
中国铬铁矿储量少产量低,分布不均衡。截止2010年,中国最大的豆荚状铬铁矿产地罗布莎已探明储量仅为5 MT左右(王希斌等, 2010)。铬铁矿的短缺使中国对外依存程度一直高居90%以上(图2)。中国豆荚状铬铁矿虽在全球重要的成矿时期均有分布,但矿床规模或铬矿含量远不及全球同期的豆荚状铬铁矿产地,如古亚洲洋域的Kempirsai和Polar Ural,中特提斯域的Vourinos和Kukes-Bulquiza-Shebenik一线,新特提斯域的Oman, Troodos, Esfandagheh等。此外,全球大型豆



中国主要的蛇绿岩带有阿尔泰带，天山-大兴安岭带，祁连-秦岭带，东-西昆仑带，班公-怒江带，雅鲁藏布带，江南带等（图中蓝色字体表示）；主要蛇绿岩型铬铁矿产地有萨尔托海，索伦，贺根山，大道尔吉，玉石沟，松树沟，东巧，罗布莎等（图中红色实心圆圈，圈的大小指示现有相对储量）。

Ophiolite belts of different ages in China: Altai, Tianshan-Daxinganling, Qilian-Qinling, Kunlun, Bangong Lake-Lujiang, Yarlung-Zangbo, Jiangnan(in blue words). Major podiform chromite deposits of China are Sartohay, Solun, Hegenshan, Dadaoerji, Yushigou, Songshugou, Dongqiao, Luobusha(the area of red filled circles means relative reserves).

图1 中国主要含矿蛇绿岩带分布地质简图  
Fig.1 Geological map, illustrating the distribution of ophiolite belts and chromite deposits with significant reserves in China (After Zhou et al., 1992; Zheng et al., 2008a; Zheng et al., 2013)



数据源于地震出版社2002-2012年《中国矿业年鉴》和姚培慧编，中国铬铁志（1996）。  
Data sources for import dependence and reserves are from 《Chinese almanac of mining》(2002-2012) and from 《Records of Chinese Chromite Deposits》(Yao Peihui., 1996).

图2 中国铬铁矿对外依存程度及主要豆荚状铬铁矿区铬铁矿储量  
Fig. 2 The import dependence and reserves of podiform chromite in China

荚状铬铁矿的著名产地还有古巴Mayarí-Baracoa蛇绿岩带，菲律宾Zambales及最年轻的新喀里多尼亚Thebaghi等（Stowe, 1994；见附表1）。

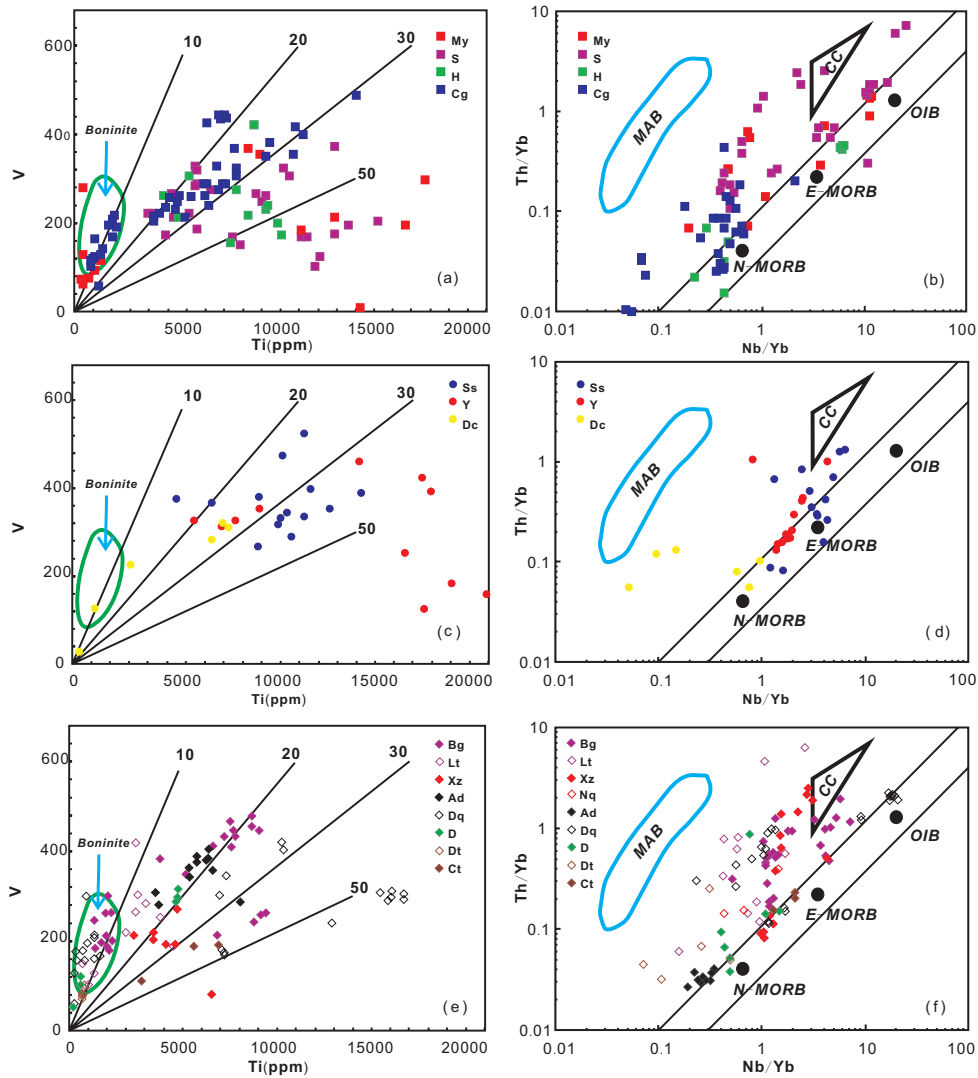
### 3 产矿蛇绿岩的构造位置

豆荚状铬铁矿中经常发现有含水硅酸盐矿物和流体包裹体（Talkington et al., 1984；Lorand

and Ceuleneer, 1989; Thalhammer et al., 1990; Mcelduff and Stumpfl, 1991; Melcher et al., 1997; Proenza et al., 1999; Al-Boghdady and Economou-Eliopoulos, 2005; Uysal et al., 2009; Rajabzadeh and Moosavinasab, 2012, 2013; Rollinson and Adetunji, 2013), 虽然此现象并非豆荚状铬铁矿特有 (Li et al., 2005; Spandler et al., 2005), 但如此丰富的富水和富碱质的包裹体可能说明了成矿母熔体具有较高的水含量, 可能是受俯冲板片的脱水作用影响, 即豆荚状铬铁矿可能的确形成于俯冲带上覆岩石圈 (简称“上俯冲带”) 这一特殊的构造

位置。

根据蛇绿岩的最新定义 (Dilek and Furnes, 2011), 雅鲁藏布蛇绿岩带 (罗布莎至东波一线) 与东地中海蛇绿岩带 (如Oman, Troodos, Shebenik, Vourinos等) 大都形成于上俯冲带环境 (Shafaii Moghadam and Stern, 2011; Hébert et al., 2012; Robertson, 2012; Shafaii Moghadam et al., 2013)。通过收集中国显生宙以来其他含矿蛇绿岩及临近蛇绿岩的基性岩微量元素数据 (附表1, 2; 图3a-f), 我们发现这些蛇绿岩投点全都位于上俯冲带区域 (Pearce et al., 1984, 2008)。



OIB: 洋岛玄武岩, N-MORB: 正常的洋脊玄武岩, E-MORB: 相对富集的洋脊玄武岩; 玻安岩(Boninite), 马里亚纳弧盆(MAB), 大陆地壳(CC)范围引自Dilek and Furnes (2011); 蛇绿岩体代号见附表1。

OIB: Ocean island basalts, N-MORB: Normal mid-ocean ridge basalts, E-MORB: Enriched mid-ocean ridge basalts; Field of Boninite, MAB: Mariana arc-basin, CC: Continental crust are from Dilek and Furnes (2011); The code name of ophiolite see in appendix 1.

图3 中国显生宙部分蛇绿岩基性岩Ti-V(a,c,e)和Nb/Yb-Th/Yb(b,d,f)图: 古亚洲洋域(a,b); 原特提斯域(c,d); 中特提斯域(e,f)  
Fig.3 Ti-V and Nb/Yb-Th/Yb discrimination diagrams for representative ophiolite suites: Paleo-Asian ophiolites (a,b); Paleo-Tethyan ophiolites (c,d); Meso-Tethyan ophiolites (e,f)

## 4 地球化学特征

### 4.1 橄榄岩全岩主量元素化学特征

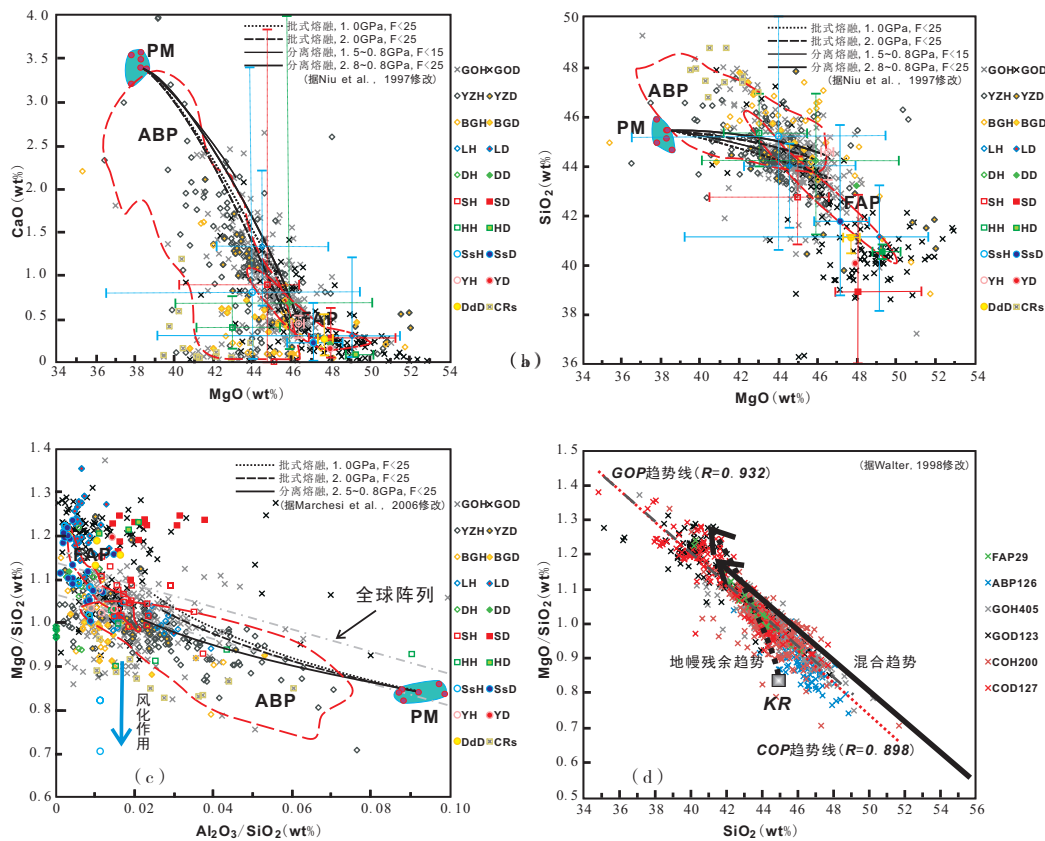
豆荚状铬铁矿多为MOHO面附近的纯橄岩所包围，常呈透镜体出现在方辉橄榄岩中。方辉橄榄岩与纯橄岩在辉石含量上逐渐过渡，说明矿体围岩经历了高程度的部分熔融和熔体-围岩反应的过程（如图4a, b），而成矿岩浆则通过纯橄岩这一岩浆通道运移集中。

从图4a-c可见，我们收集到的蛇绿岩的部分纯橄岩和方辉橄榄岩（中国除罗布莎、松树沟、萨尔托海，国外除塞浦路斯外，其他文中未明确说明是否为含矿围岩；具体数据来源见附表2）具有过高的MgO/SiO<sub>2</sub>（wt%）比值，可能说明它

们不是简单的部分熔融残余。上俯冲带蛇绿岩橄榄岩显然不符合“全球阵列”趋势（图4c；如Rollinson, 2007）。尽管可能受到蛇纹石化或海底风化作用的影响使全岩MgO含量减少（Snow and Dick., 1995; Niu, 2004），然而部分橄榄岩（方辉橄榄岩和纯橄岩，相对亏损）全岩经过无水校正后仍显示过高的MgO/SiO<sub>2</sub>比值，这可能指示蛇绿岩体橄榄岩（二辉橄榄岩或方辉橄榄岩，相对富集）在部分熔融过程中或其后有“异源富镁铁质岩浆”的加入（图4d），即后期玄武质岩浆流经时橄榄石的堆晶叠加所致（Niu, 1997, 2004）。

### 4.2 橄榄岩全岩微量元素化学特征

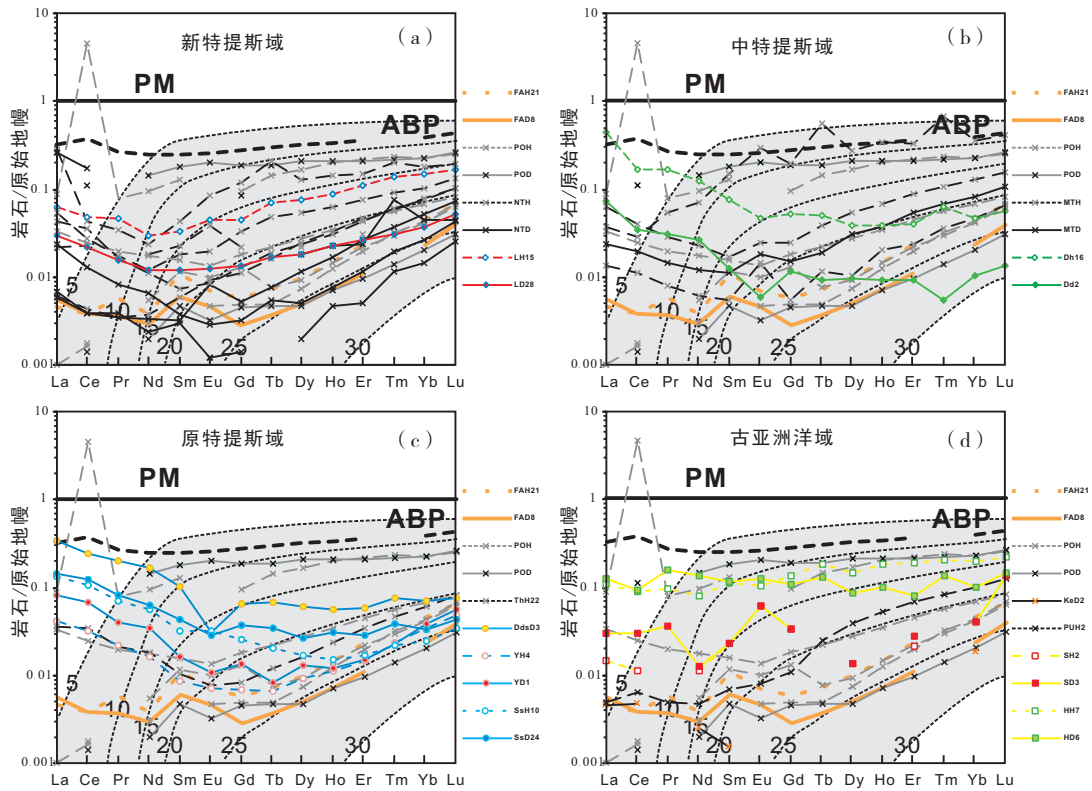
从全岩稀土元素（REE）配分模式（图5a-d；将具有相同配分模式特征的样品进行平均）可



PM: 原始地幔（数值参见Niu, 1997附录B），ABP: 全球深海橄榄岩（数据引自Niu, 2004），FAP: 弧前橄榄岩（数据引自Parkinson and Pearce, 1998），KR: 原始地幔岩成分（数值参见water, 1998）；部分熔融曲线参考文献已在图中列出；全球阵列来自Jagoutz et al. (1979) 和Hart and Zindler (1986)；图例代号表示为蛇绿岩体代号+岩性(H: 方辉橄榄岩, D: 纯橄岩, s: 蛇纹石化方辉橄榄岩), 如LH代表罗布莎方辉橄榄岩样品；GOP(全球), COP(中国)蛇绿岩体代号及具体数据来源请见附表2(其中BG代表附表2中班公湖蛇绿岩带除东巧外其他岩体, YZ代表附表2中雅鲁藏布蛇绿岩带除罗布莎外其他岩体)；所有数据统一标准化到无水总量100%。

Element concentrations are recalculated to 100% on LOI-free basis. PM, Primitive Mantle(See in appendix B of Niu, 1997). Data sources for abyssal peridotites and supra-subduction peridotites are from Niu (2004) and from Parkinson and Pearce (1998), respectively. KR: Pyrolite with the Same Composition of PM(See in Table 1 of Water, 1998)/The "terrestrial array" is from Jagoutz et al., 1979 and Hart & Zindler, 1986. The legend name is composed by the code name of ophiolite with lithology(for example: LH means Harzburgites in Luobusha). All data sources see in appendix 2.

图4 中国显生宙部分蛇绿岩橄榄岩全岩MgO-CaO(a), MgO-SiO<sub>2</sub>(b), Al<sub>2</sub>O<sub>3</sub>/SiO<sub>2</sub>-MgO/SiO<sub>2</sub> (c), SiO<sub>2</sub>-MgO/SiO<sub>2</sub> (d) 投图  
Fig.4 Bulk rock analyses for harzburgites and dunites in major podiform chromite deposits of China in spaces of MgO-CaO(a), MgO-SiO<sub>2</sub>(b), Al<sub>2</sub>O<sub>3</sub>/SiO<sub>2</sub>-MgO/SiO<sub>2</sub>(c), SiO<sub>2</sub>-MgO/SiO<sub>2</sub>(d)



原始地幔标准化数值依据Sun和McDonough (1989), 原始地幔的分离部分熔融模型图依据Niu和Hekinian (1997); 图中POH, POD (包含蛇绿岩体CR, MB, MC, TI), NTH, NTD (包含蛇绿岩体Om, Tr, Ly, An, Es), MTH, MTD (包含蛇绿岩体Pd, Ot, Vr) 分别代表附表2中全球不同时期的典型蛇绿岩体方辉橄榄岩和纯橄岩; 蛇绿岩体代号及数据来源详见附表2和附表3。

Primitive mantle-normalized values are from Sun and McDonough (1989). Fractional melting model from Niu and Hekinian (1997) is shown for comparison. POH, POD (include CR, MB, MC, TI); NTH, NTD (include Om, Tr, Ly, An, Es); MTH, MTD (include Pd, Ot, Vr) mean global typical ophiolites (Harzburgites and Dunites) of different ages. All data sources see in appendix 2 and 3.

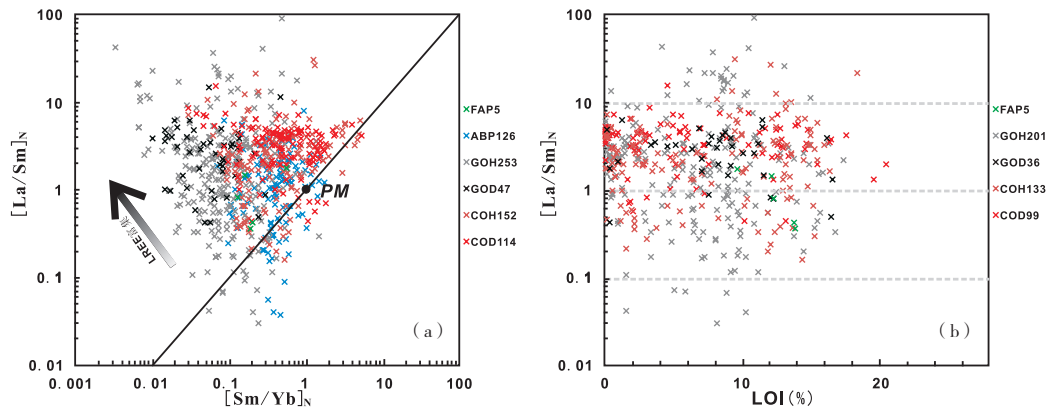
图5 中国显生宙部分蛇绿岩橄榄岩全岩稀土元素 (REE) 分配模式图  
Fig. 5 Primitive mantle-normalized REE patterns for the studied ophiolite peridotites

见, 轻稀土元素 (LREE) 相对富集, 重稀土元素 (HREE) 亏损。这并非含铬铁矿围岩或富矿蛇绿岩体中不含橄榄岩的特殊现象, 而是非常普遍, 包括全球深海橄榄岩 (Niu and Hekinian, 1997; Niu, 2004)。根据理想的部分熔融 (批式部分熔融或分离部分熔融) 模型 (即 $[La/Sm]_N$ 减小趋势应比 $[Sm/Yb]_N$ 更大),  $[La/Sm]_N$ 与 $[Sm/Yb]_N$ 投图至少应位于图6a直线下方, 但统计到的全岩REE数据均不符合这一规律, 说明LREE的富集并非是橄榄岩简单部分熔融的结果, 而是后期熔体流经早期部分熔融残余 (辉石) 时与橄榄石叠加一起富集的结果 (Niu, 2004)。Kelemen等 (1992, 1993, 1998等) 最先用熔-岩反应机制去解释岩石圈上地幔部分亏损橄榄岩样品具有高的LREE/HREE比值等特征。这一假说被很多学者引用, 以此解释蛇绿岩橄榄岩的LREE富集特征 (附表2)。

前期研究证明深海橄榄岩尽管后期遭受了较

强的蛇纹石化过程, 但LREE与高场强元素HFSE (如Nb和Zr等) 的正相关关系指示LREE与HFSE在这些橄榄岩中的富集是岩浆过程富集的结果, 而不是LREE在热液变质过程中活化叠加的结果。大量数据表明LREE在蛇纹石化过程中不具有活动性 (Niu, 2004)。最近的研究也指出上俯冲带橄榄岩的REE在蛇纹石化过程中几乎是不活动的 (Deschamps et al., 2010)。即LREE的富集很难用蛇纹石化作用解释 (如全岩烧失量与 $[La/Sm]_N$ 投图显示无相关性, 图6b)。由于统计的样品全岩REE含量较低, 暂不能排除蛇纹石化过程中热液淋滤对LREE含量的贡献 (Paulick et al., 2006), 如部分样品表现明显的Ce正异常 (如美国Coast Range 蛇绿岩带蛇纹石化方辉橄榄岩及中国东波蛇绿岩体纯橄岩) 显示了后期海水的影响。

You等 (1996) 通过模拟实验指出HFSE在俯冲带的流体中几乎是不活动的。假定LREE和



La/Sm和Sm/Yb原始地幔标准值引自Sun and McDonough (1989)；图例符号中数字代表投图所用样品个数，具体数据来源及图例解释见附表2和图4  
Primitive mantle-normalized values are from Sun and McDonough(1989). The number in the legend names mean sample amount. All data sources see in Fig. 4.

图6 全岩 $[La/Sm]_N$ - $[Sm/Yb]_N$ (a) 和  $[La/Sm]_N$ -LOI (烧失量,%) (b)投图

Fig. 6 Whole rock  $[La/Sm]_N$  vs  $[Sm/Yb]_N$  (a) and loss-on-ignition (LOI, %) (b) of the peridotites studied

HFSE在俯冲带的流体中也具有一致的地球化学行为——都不具有活动性，那么蛇绿岩橄榄岩全岩LREE与Nb、Zr等也应具有明显的正相关关系（如松树沟橄榄岩全岩LREE与Nb、Zr正相关关系明显；李犇等，2010）。然而我们注意到中国罗布莎部分含矿橄榄岩和普兰部分橄榄岩（不确定是否含矿）全岩的Zr和Nb异常富集（在收集到的全球蛇绿岩全岩LREE-HFSE投图上明显分散，区别于其他蛇绿岩体）。如果这些数据测试无误且真实地反映了全岩微量元素含量，那么可能的解释是俯冲流体对这些（含矿？）围岩的不相容元素如Zr和Nb含量有明显的贡献？此贡献过程可能类似浓度差导致的“层析”作用（非化学性质的活动）？这可能预示着还有一个更有意思的问题：为什么俯冲带流体仅影响了这些（含矿？）围岩？

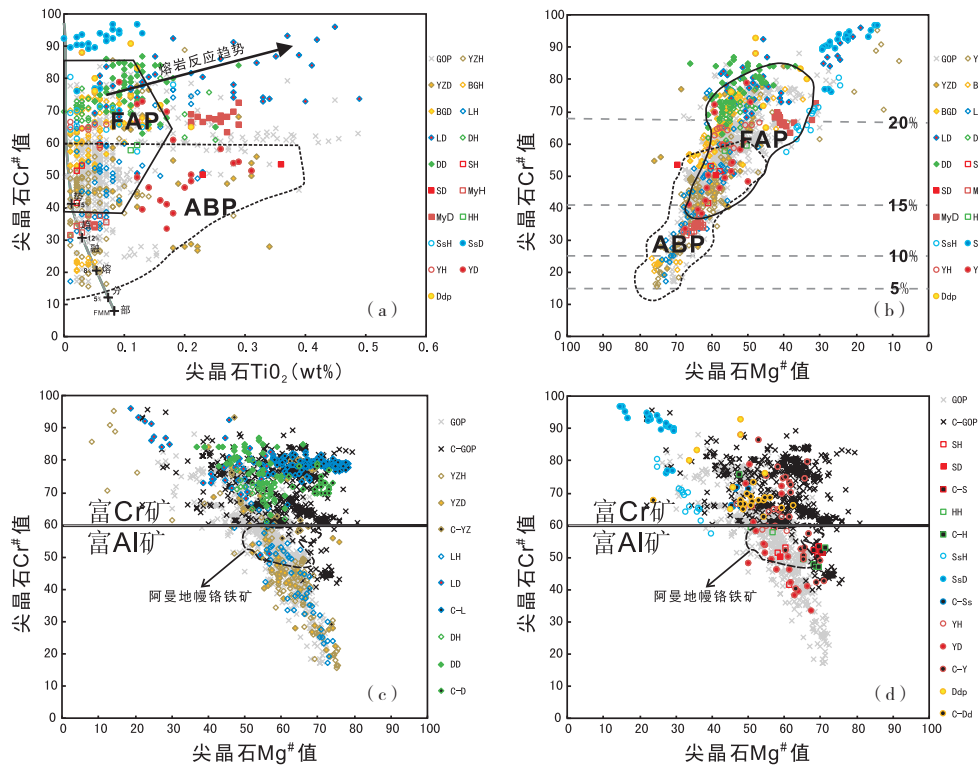
值得说明的是目前一些学者直接将“熔-岩反应”列为解释铬铁矿成因的假说之一（如Zhou and Robinson, 1994; Arai, 1997; Uysal et al., 2009; Shi et al., 2012b; 鲍佩声等, 1999; 王希斌等, 2010）。如果我们认可“熔-岩反应”包括了辉石的不一致熔融生成橄榄石这一过程： $Opx + \text{熔体}(A) \rightleftharpoons Ol + \text{熔体}(B)$ ，那么这一反应过程本身就是一个富铬的过程（熔体B比熔体A的铬含量要高）。但熔-岩反应并非含铬铁矿橄榄岩或含矿蛇绿岩体橄榄岩特有过程，这一反应并未直接导致富铬熔体的结晶聚集成矿。将“熔-岩反应”列为铬铁矿成因假说不妥，缺乏基本机制，要避免没有根据地借用。

### 4.3 尖晶石矿物化学特征

Pearce等（2000）通过上俯冲带橄榄岩的尖晶石 $TiO_2$ - $Cr^{\#}$ 投图说明经历熔-岩反应后，尖晶石 $TiO_2$ 含量会增加（图7a），而对应的铬铁矿（铬尖晶石）相对于橄榄岩铬尖晶石更富 $TiO_2$ ，故一些学者将其列为熔-岩反应促进铬铁矿形成的证据之一（如Uysal et al., 2012等）。然而作者注意到罗布莎含矿纯橄岩相对于不含矿纯橄岩，其铬尖晶石 $TiO_2$  (wt%) 较小。由于收集到的数据的限制，暂不能确定这是否是一个特例。尽管罗布莎从矿石至围岩，含矿方辉橄榄岩铬尖晶石 $TiO_2$ 含量有明显的减小趋势，但还是不能回避这样一个问题：熔-岩反应是否能导致铬铁矿的形成？两者之间可能并不存在因果关系（需要更详细的验证）。

根据收集到的蛇绿岩体橄榄岩尖晶石 $Mg^{\#}$ - $Cr^{\#}$ 投图（图7b）显示，其 $Mg^{\#}$ 和 $Cr^{\#}$ 值范围与弧前橄榄岩类似（Dick and Bullen, 1984; Barnes and Roeder, 2001）。经与对应岩体铬铁矿中铬尖晶石 $Mg^{\#}$ - $Cr^{\#}$ 投图（图7c-d），作者注意到全球蛇绿岩型铬铁矿中铬尖晶石 $Mg^{\#}$ 值范围比橄榄岩尖晶石大。收集到的数据显示中国罗布莎、东巧等地铬铁矿尖晶石 $Mg^{\#}$ 值大于对应岩体橄榄岩尖晶石，这说明铬铁矿尖晶石的结晶过程明显区别于橄榄岩尖晶石。同时也揭示出铬铁矿尖晶石在固相线下大量结晶的同时也伴随着橄榄石的结晶（ $Fe^{2+}$ 和 $Mg^{2+}$ 占据铬尖晶石晶格中的四面体位置）。

橄榄岩尖晶石的 $Cr^{\#}$ 值与橄榄岩的部分熔融程度有较好的线性关系（Dick and Bullen, 1984; Niu



$Mg^{\#} = Mg/(Mg + Fe)$ ,  $Cr^{\#} = Cr/(Cr + Al)$ ; (a)据Pearce et al., (2000) 修改, (a)(b)中深海橄榄岩(ABP)和弧前橄榄岩(FAP)范围转引Tamura et al., (2006), 部分熔融程度依据Hellebrand et al., (2001)计算, (c)(d)中阿曼地幔铬铁矿区域据Borisova et al. (2012); 图例代号第一位字母为C-蛇绿岩体代号代表对应蛇绿岩体的铬铁矿(如C-L代表罗布莎蛇绿岩体中铬铁矿), 具体蛇绿岩体代号和图例说明请见附表1和图4  $Mg^{\#} = Mg/(Mg + Fe)$ ,  $Cr^{\#} = Cr/(Cr + Al)$ . (a) modified after Pearce et al., (2000). (a)(b) Field of Abyssal Peridotites (ABP) and Fore-Arc Peridotites (FAP) are from Tamura et al. (2006); (c)(d) Field of Oman mantle chromites are from Borisova et al., (2012). The degree of melting is calculated from Hellebrand et al., 2001. The legend name is composed by Chromite (C) with the code name of ophiolite (for example: C-L means Chromites in Luobusha). All data sources see in Fig. 4.

图7 中国显生宙部分蛇绿岩橄榄岩及铬铁矿尖晶石 $TiO_2$ (wt%)— $Cr^{\#}$ 值(a)和 $Mg^{\#}$ — $Cr^{\#}$ 值(b, c, d)投图  
Fig.7 Spinel compositions in spaces of (a)  $TiO_2$ — $Cr^{\#}$  in ophiolite peridotites studied; (c, d)  $Mg^{\#}$ — $Cr^{\#}$  in spinels of the studied ophiolite chromites

and Hekinian, 1997; Hellebrand et al., 2001)。作者注意到豆荚状铬铁矿 $Cr_2O_3$ 与 $Al_2O_3$ 有良好的负相关关系(蛇绿岩型超镁铁质堆晶岩中的铬铁矿不具有此关系; Ahmed and Arai, 2002; Arai et al., 2004等)。因为在尖晶石中 $Cr^{3+}$ 比 $Al^{3+}$ 更相容, 所以随着部分熔融程度的增加, 残余尖晶石中 $Cr^{3+}/Al^{3+}$ 比值增加。亦即, 部分熔融的过程就是使尖晶石富铬的过程, 但残余尖晶石量少, 不是成矿的主要机制。也正是因为Cr是极不相容的元素, 它在原始岩浆中的含量与部分熔融的程度成正比, 而成矿Cr尖晶石是从岩浆结晶出来的, 所以“高铬(低Al)型和高铝(低Cr)型铬尖晶石分别来源于橄榄岩的高程度和低程度部分熔融产生的熔体(Zhou et al., 1994)”。因此, 原始熔体中 $Cr^{3+}$ 的含量是决定是否形成富铬矿的最直接因素。

#### 4.4 铂族元素PGE特征

铂族元素在铬铁矿矿石中主要以金属互化物形式存在, 如钨钉矿、钨铍矿等。研究显示相对于层型铬铁矿(Naldrett and Duke, 1980), 全球大多数豆荚状铬铁矿全岩的PGE原始地幔标准化分布曲线都具有不同程度的负斜率(Page et al., 1982; Zhou et al., 1998及González-Jiménez et al., 2014a, b等), 这可能是因为PPGE(Rh, Pt, Pd)和IPGE(Os, Ir, Ru)分配系数不同(Barnes et al., 1985; Bockrath et al., 2004; Righter et al., 2004); 也可能是因PGE矿物结晶期次不同(与周美夫口头交流, 2013; 熊发挥等, 2013; González-Jiménez et al., 2014a)。

PGE是一组亲硫元素, 结晶时会优先选择富硫区域(Godel et al., 2010)。实际观察发现铂族矿物(PGM)主要以合金包裹体状态赋存在铬尖晶石中, 这也为实验模拟研究(Finnigan et al.,

2008) 所证实。PGM和铬铁矿在流体相中相对于硅酸盐熔体相具有更高的结晶优越性 (Brenker et al., 2003; Okrugin, 2011), PGM在铬铁矿中的结晶过程可能与成矿熔体中硫化物的含量无关。

#### 4.5 Os同位素组成

Re-Os同位素的分馏在地幔橄榄岩中是一个很重要的岩浆过程。根据目前已发表的数据显示全球蛇绿岩型铬铁矿的 $^{187}\text{Os}/^{188}\text{Os}$ 变化范围很小 (全球蛇绿岩型铬铁矿的 $^{187}\text{Os}/^{188}\text{Os}$ 平均值 =  $0.12809 \pm 0.00085$ ; Walker et al., 2002a, 2002b), Büchl 等 (2004) 据此推算出全球蛇绿岩型铬铁矿的平均熔岩比为17:1。如果我们认可熔体渗滤过程中Os和Cr元素都相容于熔体中, 亦即铬铁矿成矿所需铬直接来源于成矿围岩发生的熔-岩反应 (Büchl et al., 2004 and therein), 那么最值得质疑的问题是含矿围岩 (未经历熔-岩反应前) 是否有足够的铬满足铬铁矿的持续结晶 (铬尖晶石的持续结晶需要的熔体/尖晶石比值为300~500; Leblanc and Ceuleneer, 1991)。

我们注意到深海橄榄岩全岩Os同位素组成可能受到海水的影响 (Snow and Reisberg, 1995; Alard et al., 2005), 变质热液流体也能对铬铁矿中铂族硫化物的Os同位素组成产生影响 (González-Jiménez et al., 2012a)。最近的研究 (González-Jiménez et al., 2012b) 显示Os同位素组成在铬铁矿铂族硫化物中的分布具有不均一性, 故我们不得不谨慎对待测试到的铬铁矿全岩或铬尖晶石Os同位素组成 (可能只代表了平均值)。González-Jiménez等 (2012b) 认为Os同位素组成的不均一特征是由铬铁矿形成时受到不同成分熔体扰动 (熔-岩反应或熔体混合) 导致的, 此项研究同时也说明古巴Mayarí-Baracoa 蛇绿岩带Sagua de Tánamo岩体中参与熔-岩反应的熔体并不仅仅来源于赋矿围岩。

## 5 蛇绿岩型铬铁矿成矿过程的一些思考

前人研究提出铬铁矿结晶主要与温度 (Ballhaus et al., 1991等), 压力 (Dick and Bullen, 1984等), 氧逸度 (Ulmer, 1969等), 熔体成分 (Irvine, 1976等) 等因素有关。熔-岩反

应假说有助于我们理解铬铁矿的成因, 但此反应没有成矿元素真正富集成矿的机制。

### 5.1 水对豆荚状铬铁矿形成的作用

Matveev和Ballhaus (2002) 的模拟实验研究指出豆荚状铬铁矿铬尖晶石的结晶并不需要抑制橄榄石的结晶。他们推断铬尖晶石在流体 (水) 中具有相对较高的结晶优势能。这一观点启发我们去思考水在铬铁矿形成过程中所扮演的具体角色。高含量水的存在不仅促进了橄榄岩的部分熔融, 亦即促进辉石中Cr的释放; 同时由于抑制了熔体中硅酸盐格架的形成 (Edwards et al., 2000 and therein), 从而 $\text{Cr}^{3+}$ 会优先占据铬尖晶石八面体晶格位置。不同成分的熔体混合 (不混溶) 会促进富Cr熔体在富镁铁质区域聚集 (Edwards, 1995; Ballhaus, 1998)。如果水在富铬熔体的迁移集中过程扮演了搬运介质的角色 (Matveev and Ballhaus, 2002), 那就不能忽略这些流体 (水) 对成矿围岩及矿石微量元素的贡献 (罗布莎, 普兰, 东波等岩体成矿围岩与铬铁矿石全岩REE均具有U型特征; 附表2文献)。

Zhou等 (2001b) 提出的铬铁矿成矿模式同样能解释豆荚状结构铬铁矿的形成过程。González-Jiménez等 (2014b) 同样强调了不同来源的熔浆混合过程对铬铁矿形成的重要性。铬铁矿的形成需要铬尖晶石集中分离结晶, 但以上成矿模式在回答铬尖晶石为什么在一定部位大量结晶成矿这一关键问题上模糊的。目前的认识是铬铁矿矿体的分布受到前期形成的断裂带的控制。为什么豆荚状矿体是不连续分布的? 矿石围岩铬尖晶石为什么与铬铁矿铬尖晶石化学成分有很大差别 (如 $\text{TiO}_2$ ,  $\text{Mg}^\#$ )? 我们希望通过同一矿体区域周围的含矿围岩和不含矿围岩进行空间上温度、氧逸度等物理因素的估算对比来找到答案。

### 5.2 铬铁矿石包裹体的启示

硅酸盐矿物包裹体在蛇绿岩型铬铁矿石矿物颗粒间和矿物内部大量存在, 其成分代表了铬铁矿结晶时的伴生熔体成分。我们注意到蛇绿岩型豆荚状铬铁矿 (矿石为豆荚状结构) 的硅酸盐包裹体含量明显大于层状或似层状铬铁矿 (矿石为条带状或浸染状结构) (Lorand and Ceuleneer, 1989), 这可能是由地幔流动产生的热变形造成

的。那么这种热变形是否对铬铁矿矿石结构及矿体整体Cr含量产生了影响?

近年来相继在罗布莎、泽当、日喀则、当穷、普兰和东波等蛇绿岩的橄榄岩矿物颗粒间、铬铁矿矿物颗粒间、铬铁矿铂族矿物包裹体中发现金刚石等超高压矿物(Yang et al., 2007; 杨经绥等, 2011, 2013), 这可能说明成矿物质Cr不仅来源于成矿围岩辉石不一致部分熔融, 也许还有来自更深源区的富镁铁质熔体的贡献(Arai, 2010, 2013)。那么上俯冲带蛇绿岩及其所含金刚石等超高压矿物是否能给予我们更多的信息?

## 6 小结

1) 前人的研究促进了我们对蛇绿岩型铬铁矿形成过程的认识, 但并未直接回答铬铁矿如何形成这一问题。铬铁矿体的形成至少需要以下3个步骤: (1) 熔体获得较高的Cr含量; (2) 富Cr熔体区域聚集; (3) 聚集的富铬熔体大量分离结晶形成铬铁矿体。铬铁矿床的形成需要经历铬元素的富集过程。如果我们认可蛇绿岩型铬铁矿成矿元素Cr的主要来源是矿体周围橄榄岩的部分熔融, 那么具有较大体积纯橄岩相的东波、普兰、当穷等蛇绿岩体具有很大的找矿前景。

2) 熔-岩反应是否导致了Cr的活化? 熔-岩反应与铬铁矿的形成是因果关系还是两个独立的岩浆过程? 含矿纯橄岩微量元素特征(如LREE和Zr, Nb等富集)是由熔-岩反应导致还是其他因素(蛇纹石化、流体等)? 回答这些问题需要我们对同一矿体区域周围的含矿围岩和不含矿围岩进行详细的岩石学和地球化学特征对比研究。

3) 蛇绿岩型铬铁矿中豆荚状铬铁矿体和条带状、浸染状铬铁矿体可同时存在, 它们是否具有相同的成矿过程? 铬铁矿体可同时赋存在蛇绿岩地幔橄榄岩和下地壳超镁铁质堆晶岩中(如大道尔吉), 它们的成矿元素Cr是否都来源于围岩? 对这些问题的思考将有助于我们发现真正的“找矿标志”(非经验总结)。

4) 综上所述, 全球上俯冲带蛇绿岩“壳-幔”过渡带均具有铬铁矿化, 说明豆荚状铬铁矿化的普遍性, 但不一定总是形成客观的大矿、富矿, 说明在这些蛇绿岩体系里不存在缺乏金属量

的问题, 而是需要金属富集的特殊机制。后者是我们继续研究的核心。

**致谢:** 本工作受中国地质调查局地质调查项目(编号: 1212011121092, 1212011220928)资助。论文成文过程中与铬铁矿研究相关科研人员及一线地质工作者进行了有益探讨, 在此一并表示感谢。

## 参考文献 (References):

- 鲍佩声, 王希斌, 彭根永, 等. 1999. 中国铬铁矿床[M]. 北京: 科学出版社: 143-297.
- 黄圭成, 徐德明, 雷义均, 等. 2007. 西藏西南部达巴-休古嘎布绿岩带铬铁矿的找矿前景[J]. 中国地质, 34(4): 668-674.
- 李桦, 朱赖民, 弓虎军, 等. 2010. 北秦岭松树沟橄榄岩与铬铁矿床的成因关系[J]. 岩石学报, 26(5): 1487-1502.
- 李军, 陈强, 赵献军, 等. 2012. 库地铬铁矿地质特征及西昆仑北蛇绿岩带铬铁矿成矿远景探讨[J]. 新疆地质, 30(3): 304-306.
- 王希斌, 周详, 郝梓国. 2010. 西藏罗布莎铬铁矿床的进一步找矿意见和建议[J]. 地质通报, 29(1): 105-114.
- 熊发挥, 杨经绥, 刘钊. 2013. 豆荚状铬铁矿多阶段形成过程的讨论[J]. 中国地质, 40(3): 820-839.
- 杨经绥, 熊发挥, 郭国林, 等. 2011. 东波超镁铁岩体: 西藏雅鲁藏布江缝合带西段一个甚具铬铁矿前景的地幔橄榄岩体[J]. 岩石学报, 27(11): 3207-3222.
- 杨经绥, 徐向珍, 戎合, 等. 2013. 蛇绿岩地幔橄榄岩中的深部矿物: 发现与研究进展[J]. 矿物岩石地球化学通报, 32(2): 159-170.
- 姚培慧. 1996. 中国铬矿志[M]. 北京: 冶金工业出版社: 1-23.
- Ahmed A H and Arai S. 2002. Unexpectedly high-PGE chromitite from the deeper mantle section of the northern Oman ophiolite and its tectonic implications [J]. Contributions to Mineralogy and Petrology, 143: 263-278.
- Alard O, Luguet A, Pearson N J, et al. 2005. In situ Os isotopes in abyssal peridotites bridge the isotopic gap between MORBs and their source mantle [J]. Nature, 436: 1005-1008.
- Al-Boghdady A and Economou-Eliopoulos M. 2005. Fluid inclusions in chromite from a pyroxenite dike of the Pindos ophiolite complex [J]. Chemie der Erde-Geochemistry, 65: 191-202.
- Arai S and Yurimoto H. 1994. Podiform chromitites of the Tari-Misaka ultramafic complex, southwestern Japan, as mantle-melt interaction products [J]. Economic Geology, 89: 1279-1288.
- Arai S. 1997. Origin of podiform chromitites [J]. Journal of Asian Earth Sciences, 15: 303-310.
- Arai S, Uesugi J and Ahmed A H. 2004. Upper crustal podiform chromitite from the northern Oman ophiolite as the stratigraphically shallowest chromitite in ophiolite and its implication for Cr concentration [J]. Contributions to Mineralogy and Petrology, 147: 145-154.
- Arai S. 2010. Possible recycled origin for ultrahigh-pressure chromitites in ophiolites [J]. Journal of mineralogical and petrological sciences, 105: 280-285.
- Arai S. 2013. Conversion of low-pressure chromitites to ultrahigh-pressure chromitites by deep recycling: A good inference [J]. Earth and Planetary Science Letters, 379: 81-87.
- Ballhaus C, Berry R F and Green D H. 1991. High pressure experimental calibration of the olivine-orthopyroxene-spinel oxygen

- geobarometer: implications for the oxidation state of the upper mantle [J]. *Contributions to Mineralogy and Petrology*, 107: 27–40.
- Ballhaus C. 1998. Origin of podiform chromite deposits by magma mingling [J]. *Earth and Planetary Science Letters*, 156: 185–193.
- Barnes S J and Roeder P L. 2001. The range of spinel compositions in terrestrial mafic and ultramafic rocks [J]. *Journal of Petrology*, 42: 2279–2302.
- Barnes S J, Naldrett A J and Gorton M P. 1985. The origin of the fractionation of platinum-group elements in terrestrial magmas [J]. *Chemical Geology*, 53: 303–323.
- Bockrath C, Ballhaus C and Holzheid A. 2004. Fractionation of the platinum-group elements during mantle melting [J]. *Science*, 305: 1951–1953.
- Brenker F E, Meibom A and Frei R. 2003. On the formation of peridotite-derived Os-rich PGE alloys [J]. *American Mineralogist*, 88: 1731–1740.
- Büchl A, Brügmann G and Batanova V G. 2004. Formation of podiform chromitite deposits: implications from PGE abundances and Os isotopic compositions of chromites from the Troodos complex, Cyprus [J]. *Chemical geology*, 208: 217–232.
- Caran S, Coban H, Flower M F J, et al. 2010. Podiform chromitites and mantle peridotites of the Antalya ophiolite, Isparta Angle (SW Turkey): Implications for partial melting and melt-rock interaction in oceanic and subduction-related settings [J]. *Lithos*, 114: 307–326.
- Cassard D, Nicolas A, Rabinovitch M, et al. 1981. Structural classification of chromite pods in southern New Caledonia [J]. *Economic Geology*, 76: 805–831.
- Deschamps F, Guillot S, Godard M, et al. 2010. In situ characterization of serpentinites from forearc mantle wedges: Timing of serpentinitization and behavior of fluid-mobile elements in subduction zones [J]. *Chemical Geology*, 269: 262–277.
- Dick H J B and Bullen T. 1984. Chromian spinel as a petrogenetic indicator in abyssal and alpine-type peridotites and spatially associated lavas [J]. *Contributions to Mineralogy and Petrology*, 86: 54–76.
- Dilek Y and Furnes H. 2011. Ophiolite genesis and global tectonics: Geochemical and tectonic fingerprinting of ancient oceanic lithosphere [J]. *Geological Society of America Bulletin*, 123: 387–411.
- Edwards S J, Pearce J A and Freeman J. 2000. New insights concerning the influence of water during the formation of podiform chromitite [C] // Dilek Y, Moores E, Elthon D. and Nicolas A. (Eds.) *Ophiolites and Oceanic Crust: New Insights from Field Studies and the Ocean Drilling Program*. Geological Society of America, Special Paper, 349: 139–147.
- Edwards S J. 1995. Boninitic and tholeiitic dykes in the Lewis Hills mantle section of the Bay of Islands ophiolite: implications for magmatism adjacent to a fracture zone in a back-arc spreading environment [J]. *Canadian Journal of Earth Sciences*, 32: 2128–2146.
- Finnigan C S, Brennan J M, Mungall J E, et al. 2008. Experiments and models bearing on the role of chromite as a collector of platinum group minerals by local reduction [J]. *Journal of Petrology*, 49: 1647–1665.
- Godel B, Barnes S J, Barnes S-J, et al. 2010. Platinum ore in three dimensions: Insights from high-resolution X-ray computed tomography [J]. *Geology*, 38: 1127–1130.
- González-Jiménez J M, Proenza J A, Gervilla F, et al. 2011. High-Cr and high-Al chromitites from the Sagua de T ú namo district, Mayarí - Cristal Ophiolitic Massif (eastern Cuba): constraints on their origin from mineralogy and geochemistry of chromian spinel and platinum-group elements [J]. *Lithos*, 125: 101–121.
- González-Jiménez J M, Griffin W L, Gervilla F, et al. 2012a. Metamorphism disturbs the Re-Os signatures of platinum-group minerals in ophiolite chromitites [J]. *Geology*, 40: 659–662.
- González-Jiménez J M, Gervilla F, Griffin W L, et al. 2012b. Os-isotope variability within sulfides from podiform chromitites [J]. *Chemical Geology*, 291: 224–235.
- González-Jiménez J M, Griffin W L, Gervilla F, et al. 2014a. Chromitites in ophiolites: How, where, when, why? Part I. A review and new ideas on the origin and significance of platinum-group minerals [J]. *Lithos*, 189: 127–139.
- González-Jiménez, J M, Griffin, W L, Proenza, J A, et al, 2014b. Chromitites in ophiolites: how, where, when, why? Part II. The crystallisation of chromitites [J]. *Lithos*, 189: 140–158.
- Hart S R and Zindler A. 1986. In search of a bulk-Earth composition [J]. *Chemical Geology*, 57: 247–267.
- Hébert R, Bezard R, Guilmette C, et al. 2012. The Indus-Yarlung Zangbo ophiolites from Nanga Parbat to Namche Barwa syntaxes, southern Tibet: First synthesis of petrology, geochemistry, and geochronology with incidences on geodynamic reconstructions of Neo-Tethys [J]. *Gondwana Research*, 22: 377–397.
- Hellebrand E, Snow J E, Dick H J, et al. 2001. Coupled major and trace elements as indicators of the extent of melting in mid-ocean-ridge peridotites [J]. *Nature*, 410: 677–681.
- Irvine T N. 1976. Chromite crystallisation in the join  $Mg_2SiO_4$ – $CaMgSi_2O_6$ – $CaAl_2Si_2O_8$ – $MgCr_2O_4$ – $SiO_2$  [G]. *Carnegie Institution of Washington Year book*, 76: 465–472.
- Irvine T N. 1977. Origin of chromitite layers in the Muskox intrusion and other stratiform intrusions: A new interpretation [J]. *Geology*, 5: 273–277.
- Jagoutz E, Palme H, Baddenhausen H, et al. 1979. The abundances of major, minor and trace elements in the earth's mantle as derived from primitive ultramafic nodules [J]. *Proceedings of 10th Lunar Planetary Science Conference*. *Geochimica et Cosmochimica Acta Supplements*, 10: 2031–2051.
- Kelemen P B, Dick H J and Quick J E. 1992. Formation of harzburgite by pervasive melt/rock reaction in the upper mantle [J]. *Nature*, 358: 635–641.
- Kelemen P B, Shimizu N and Dunn T. 1993. Relative depletion of niobium in some arc magmas and the continental crust: partitioning of K, Nb, La and Ce during melt/rock reaction in the upper mantle [J]. *Earth and Planetary Science Letters*, 120: 111–134.
- Kelemen P B, Hart S R and Bernstein S. 1998. Silica enrichment in the continental upper mantle via melt/rock reaction [J]. *Earth and Planetary Science Letters*, 164: 387–406.
- Leblanc M and Ceuleneer G. 1991. Chromite crystallization in a multicellular magma flow: evidence from a chromitite dike in the Oman ophiolite [J]. *Lithos*, 27: 231–257.
- Li C, Ripley E M, Sarkar A, et al. 2005. Origin of phlogopite-orthopyroxene inclusions in chromites from the Merensky Reef of the Bushveld Complex, South Africa [J]. *Contributions to Mineralogy and Petrology*, 150: 119–130.

- Lorand J P and Ceuleneer G. 1989. Silicate and base-metal sulfide inclusions in chromites from the Maqсад area (Oman ophiolite, Gulf of Oman): a model for entrapment [J]. *Lithos*, 22: 173–190.
- Marchesi C, Garrido C J, Godard M, et al. 2006. Petrogenesis of highly depleted peridotites and gabbroic rocks from the Mayarí–Baracoa Ophiolitic Belt (eastern Cuba) [J]. *Contributions to Mineralogy and Petrology*, 151: 717–736.
- Matveev S and Ballhaus C. 2002. Role of water in the origin of podiform chromitite deposits [J]. *Earth and Planetary Science Letters*, 203: 235–243.
- Mcelduff B and Stumpf E F. 1991. The chromite deposits of the Troodos complex, Cyprus: evidence for the role of a fluid phase accompanying chromite formation [J]. *Mineralium Deposita*, 26: 307–318.
- Melcher F, Grum W, Simon G, et al. 1997. Petrogenesis of the ophiolitic giant chromite deposits of Kempirsai, Kazakhstan: a study of solid and fluid inclusions in chromite [J]. *Journal of Petrology*, 38: 1419–1458.
- Metcalf I. 2013. Gondwana dispersion and Asian accretion: Tectonic and palaeogeographic evolution of eastern Tethys [J]. *Journal of Asian Earth Sciences*, 66: 1–33.
- Naldrett A J and Duke J M. 1980. Platinum metals magmatic sulfide ores [J]. *Science*, 208: 1417–1424.
- Niu Y L and Hérninian R. 1997. Basaltic liquids and harzburgitic residues in the Garrett Transform: a case study at fast-spreading ridges [J]. *Earth and Planetary Science Letters*, 146: 243–258.
- Niu Y L. 1997. Mantle melting and melt extraction processes beneath ocean ridges: evidence from abyssal peridotites [J]. *Journal of Petrology*, 38: 1047–1074.
- Niu Y L. 2004. Bulk-rock major and trace element compositions of abyssal peridotites: implications for mantle melting, melt extraction and post-melting processes beneath mid-ocean ridges [J]. *Journal of Petrology*, 45: 2423–2458.
- Niu Y L, Langmuir C H and Kinzler R J. 1997. The origin of abyssal peridotites: a new perspective [J]. *Earth and Planetary Science Letters*, 152: 251–265.
- Okrugin A V. 2011. Origin of platinum group minerals in mafic and ultramafic rocks: from dispersed elements to nuggets [J]. *The Canadian Mineralogist*, 49: 1397–1412.
- Page N J, Cassard D and Haffty J. 1982. Palladium, platinum, rhodium, ruthenium, and iridium in chromites from the Massif du Sud and Tiebaghi Massif, New Caledonia [J]. *Economic Geology*, 77: 1571–1577.
- Paktunc A D. 1990. Origin of podiform chromite deposits by multistage melting, melt segregation and magma mixing in the upper mantle [J]. *Ore Geology Reviews*, 5: 211–222.
- Parkinson I J and Pearce J A. 1998. Peridotites from the Izu–Bonin–Mariana forearc (ODP Leg 125): evidence for mantle melting and melt-mantle interaction in a supra-subduction zone setting [J]. *Journal of Petrology*, 39: 1577–1618.
- Paulick H, Bach W, Godard M, et al. 2006. Geochemistry of abyssal peridotites (Mid-Atlantic Ridge, 15° 20'N, ODP Leg 209): implications for fluid/rock interaction in slow spreading environments [J]. *Chemical Geology*, 234: 179–210.
- Pearce J A, Lippard S J and Roberts S. 1984. Characteristics and tectonic significance of supra-subduction zone ophiolites [J]. *Geological Society, London, Special Publications*, 16: 77–94.
- Pearce J A. 2008. Geochemical fingerprinting of oceanic basalts with applications to ophiolite classification and the search for Archean oceanic crust [J]. *Lithos*, 100: 14–48.
- Pearce J A, Barker P F, Edwards S J, et al. 2000. Geochemistry and tectonic significance of peridotites from the South Sandwich arc–basin system, South Atlantic [J]. *Contributions to Mineralogy and Petrology*, 139: 36–53.
- Proenza J, Gervilla F, Melgarejo J, et al. 1999. Al- and Cr-rich chromitites from the Mayarí–Baracoa ophiolitic belt (eastern Cuba): consequence of interaction between volatile-rich melts and peridotites in suprasubduction mantle [J]. *Economic Geology*, 94: 547–566.
- Rajabzadeh M A and Moosavinasab Z. 2012. Mineralogy and distribution of Platinum-Group Minerals (PGM) and other solid inclusions in the Neyriz ophiolitic chromitites, Southern Iran [J]. *The Canadian Mineralogist*, 50: 643–665.
- Rajabzadeh M A and Moosavinasab Z. 2013. Mineralogy and distribution of Platinum-Group Minerals (PGM) and other solid inclusions in the Faryab ophiolitic chromitites, Southern Iran [J]. *Mineralogy and Petrology*, 107: 943–962.
- Righter K, Campbell A J, Humayun M, et al. 2004. Partitioning of Ru, Rh, Pd, Re, Ir, and Au between Cr-bearing spinel, olivine, pyroxene and silicate melts [J]. *Geochimica et Cosmochimica Acta*, 68: 867–880.
- Roberts S and Neary C. 1993. Petrogenesis of ophiolitic chromitite [J]. *Geological Society, London, Special Publications*, 76: 257–272.
- Robertson A H. 2012. Late Palaeozoic–Cenozoic tectonic development of Greece and Albania in the context of alternative reconstructions of Tethys in the Eastern Mediterranean region [J]. *International Geology Review*, 54: 373–454.
- Robinson P T, Zhou M F, Malpas J, et al. 1997. Podiform chromitites: Their composition, origin and environment of formation [J]. *Episodes*, 20: 247–252.
- Robinson P T, Bai W J, Malpas J, et al. 2004. Ultra-high pressure minerals in the Luobusa Ophiolite, Tibet, and their tectonic implications [J]. *Geological Society, London, Special Publications*, 226: 247–271.
- Rollinson H. 2007. Recognising early Archean mantle: a reappraisal [J]. *Contributions to Mineralogy and Petrology*, 154: 241–252.
- Rollinson H and Adetunji J. 2013. Mantle podiform chromitites do not form beneath mid-ocean ridges: A case study from the Moho transition zone of the Oman ophiolite [J]. *Lithos*, 177: 314–327.
- Shafaii Moghadam H, Corfu F and Stern R J. 2013. U–Pb zircon ages of Late Cretaceous Nain–Dehshir ophiolites, central Iran [J]. *Journal of the Geological Society*, 170: 175–184.
- Shafaii Moghadam H and Stern R J. 2011. Geodynamic evolution of Upper Cretaceous Zagros ophiolites: formation of oceanic lithosphere above a nascent subduction zone [J]. *Geological Magazine*, 148: 762–801.
- Shi R D, Alard O, Zhi X C, et al. 2007. Multiple events in the Neo-Tethyan oceanic upper mantle: evidence from Ru–Os–Ir alloys in the Luobusa and Dongqiao ophiolitic podiform chromitites, Tibet [J]. *Earth and Planetary Science Letters*, 261: 33–48.
- Shi R D, Griffin W L, O'Reilly S Y, et al. 2012a. Melt/mantle mixing produces podiform chromite deposits in ophiolites: Implications of Re–Os systematics in the Dongqiao Neo–Tethyan ophiolite, northern Tibet [J]. *Gondwana Research*, 21: 194–206.
- Shi R D, Griffin W L, O'Reilly S Y, et al. 2012b. Archean mantle

- contributes to the genesis of chromitite in the Palaeozoic Sartohay ophiolite, Asiatic Orogenic Belt, northwestern China [J]. *Precambrian Research*, 216–219: 87–94.
- Snow J E and Dick H J. 1995. Pervasive magnesium loss by marine weathering of peridotite [J]. *Geochimica et Cosmochimica Acta*, 59: 4219–4235.
- Snow J E and Reisberg L. 1995. Os isotopic systematics of the MORB mantle: results from altered abyssal peridotites [J]. *Earth and Planetary Science Letters*, 133: 411–421.
- Spandler C, Mavrogenes J and Arculus R. 2005. Origin of chromitites in layered intrusions: Evidence from chromite-hosted melt inclusions from the Stillwater Complex [J]. *Geology*, 33: 893–896.
- Stampfli G M and Borel G D. 2002. A plate tectonic model for the Paleozoic and Mesozoic constrained by dynamic plate boundaries and restored synthetic oceanic isochrones [J]. *Earth and Planetary Science Letters*, 196: 17–33.
- Stowe C W. 1994. Compositions and tectonic settings of chromite deposits through time [J]. *Economic Geology*, 89: 528–546.
- Sun S-s and McDonough W F. 1989. Chemical and isotopic systematics of ocean basalt: Implications for mantle composition and processes [A]. //A.D. Saunders and Norry M J(Eds.), *Magmatism of the Ocean Basins*. Geological Society of London Special Publication, 42: 323–345.
- Talkington R W, Watkinson D H, Whittaker P J, et al. 1984. Platinum-group minerals and other solid inclusions in chromite of ophiolitic complexes: occurrence and petrological significance [J]. *Mineralogy and Petrology*, 32: 285–301.
- Tamura A and Arai S. 2006. Harzburgite–dunite–orthopyroxenite suite as a record of supra-subduction zone setting for the Oman ophiolite mantle [J]. *Lithos*, 90: 43–56.
- Thalhammer O, Prochaska W and Mühlhans H W. 1990. Solid inclusions in chrome-spinels and platinum group element concentrations from the Hochgrößen and Kraubath Ultramafic Massifs (Austria) [J]. *Contributions to Mineralogy and Petrology*, 105: 66–80.
- Ulmer G C. 1969. Experimental investigations of chromite spinels [J], in: Wilson, H.D.B. (Eds.), *Magmatic ore deposits*. *Economic Geology Monograph*, 4: 114–131.
- Uysal i M, Kaliwoda M, Karsli O, et al. 2007. Compositional variations as a result of partial melting and melt-peridotite interaction in an upper mantle section from the Ortaca area, southwestern Turkey [J]. *The Canadian Mineralogist*, 45: 1471–1493.
- Uysal i M, Tarkian M, Sadiklar M B, et al. 2009. Petrology of Al- and Cr-rich ophiolitic chromitites from the Muğla, SW Turkey: implications from composition of chromite, solid inclusions of platinum-group mineral, silicate, and base-metal mineral, and Os-isotope geochemistry [J]. *Contributions to Mineralogy and Petrology*, 158: 659–674.
- Uysal i M, Ersoy E Y, Karsli O, et al. 2012. Coexistence of abyssal and ultra-depleted SSZ type mantle peridotites in a Neo-Tethyan Ophiolite in SW Turkey: Constraints from mineral composition, whole-rock geochemistry (major-trace-REE-PGE), and Re–Os isotope systematics [J]. *Lithos*, 132–133: 50–69.
- Walker R J, Prichard H M, Ishiwatari A, et al. 2002a. The osmium isotopic composition of the convecting upper mantle deduced from ophiolite chromites [J]. *Geochimica et Cosmochimica Acta*, 66: 329–345.
- Walker R J, Horan M F, Morgan J W, et al. 2002b. Comparative  $^{187}\text{Re}$ – $^{187}\text{Os}$  systematics of chondrites: implications regarding early solar system processes [J]. *Geochimica et Cosmochimica Acta*, 66: 4187–4201.
- Yamamoto S, Komiya T, Hirose K, et al. 2009. Coesite and clinopyroxene exsolution lamellae in chromites: In-situ ultrahigh-pressure evidence from podiform chromitites in the Luobusa ophiolite, southern Tibet [J]. *Lithos*, 109: 314–322.
- Yang J S, Dobrzhinetskaya L, Bai W J, et al. 2007. Diamond- and coesite-bearing chromitites from the Luobusa ophiolite, Tibet [J]. *Geology*, 35: 875–878.
- Yang J S, Bai W J, Dobrzhinetskaya L, et al. 2009. In situ diamonds in polished chromitite fragments from the chromite deposits in Polar Ural and Tibet [J], *Eos, Trans. AGU*, 90 ( 52), Fall Meeting Supplement Abstracts, 54: 08.
- You C F, Castillo P R, Gieskes J M, et al. 1996. Trace element behavior in hydrothermal experiments: Implications for fluid processes at shallow depths in subduction zones [J]. *Earth and Planetary Science Letters*, 140: 41–52.
- Zhang H F, Goldstein S L, Zhou X H, et al. 2008a. Evolution of subcontinental lithospheric mantle beneath eastern China: Re–Os isotopic evidence from mantle xenoliths in Paleozoic kimberlites and Mesozoic basalts [J]. *Contributions to Mineralogy and Petrology*, 155: 271–293.
- Zhang Q, Wang C Y, Liu D Y, et al. 2008b. A brief review of ophiolites in China [J]. *Journal of Asian Earth Sciences*, 32: 308–324.
- Zheng Y F, Xiao W J and Zhao G C. 2013. Introduction to tectonics of China [J]. *Gondwana Research*, 23: 1189–1206.
- Zhou M F and Bai W J. 1992. Chromite deposits in China and their origin [J]. *Mineralium Deposita*, 27: 192–199.
- Zhou M F and Robinson P T. 1994. High-Cr and high-Al podiform chromitites, Western China: relationship to partial melting and melt/rock reaction in the upper mantle [J]. *International Geology Review*, 36: 678–686.
- Zhou M F, Robinson P T and Bai W J. 1994. Formation of podiform chromitites by melt/rock interaction in the upper mantle [J]. *Mineralium Deposita*, 29: 98–101.
- Zhou M F, Robinson P T, Malpas J, et al. 1996. Podiform chromitites in the Luobusa ophiolite (southern Tibet): Implications for melt-rock interaction and chromite segregation in the upper mantle [J]. *Journal of Petrology*, 37: 3–21.
- Zhou M F and Robinson P T. 1997. Origin and tectonic environment of podiform chromite deposits [J]. *Economic Geology*, 92: 259–262.
- Zhou M F, Sun M, Keays R R, et al. 1998. Controls on platinum-group elemental distributions of podiform chromitites: a case study of high-Cr and high-Al chromitites from Chinese orogenic belts [J]. *Geochimica et Cosmochimica Acta*, 62: 677–688.
- Zhou M F, Robinson P T, Malpas J, et al. 2001a. Melt/mantle interaction and melt evolution in the Sartohay high-Al chromite deposits of the Dalabute ophiolite (NW China) [J]. *Journal of Asian Earth Sciences*, 19: 517–534.
- Zhou M F, Malpas J, Robinson P T, et al. 2001b. Crystallization of podiform chromitites from silicate magmas and the formation of nodular textures [J]. *Resource Geology*, 51: 1–6.

附表1 中国显生宙典型造山带蛇绿岩及全球主要含矿蛇绿岩年龄统计表

蛇绿岩名称及代号	定年样品	定年方法	年龄(Ma)	年龄来源	基性岩数据来源
<b>古亚洲洋域 (Paleo-Asian ophiolites)</b>					
哈萨克斯坦Kempirsai(Ke)	辉长岩	全岩Sm-Nd	400~420	Melcher et al., 1999	
俄罗斯Polar Ural(Pu)	硬玉岩	锆石 U-Pb	404 ± 7	Meng et al., 2011	
*萨尔托海Sartuohay(S)	辉长岩	全岩Sm-Nd	395 ± 12	张弛等, 1992	
	辉长岩	锆石 U-Pb	391.1 ± 6.8	辜平阳等, 2009	
	辉长岩	锆石 U-Pb	302.5 ± 1.7	刘希军等, 2009	Yang et al., 2012(JAES)
	辉长岩	锆石 U-Pb	391 ± 6	Yang et al., 2012(GR)	
	辉长岩	锆石 U-Pb	426 ± 6	陈石等, 2010	
*玛依勒Mayile(My)	碱性玄武岩	全岩 Rb-Sr	435.3 ± 6.5	魏荣珠, 2010	Yang et al., 2012(Lithos); Zhao et al., 2012; Zhang et al., 2011
	基性熔岩	全岩 Rb-Sr	~421	朱荣清等, 1987	
	辉长岩	锆石 U-Pb	572 ± 9	Yang et al., 2012(Lithos)	
*洪古勒楞Hongguleleng(Hg)	堆晶岩	全岩Sm-Nd	444 ± 27	张弛等, 1992	
	钙长岩	锆石 U-Pb	~475		
	辉长岩	锆石 U-Pb	409 ± 23	Jian et al., 2005	
	辉长岩	锆石 U-Pb	472 ± 8.4	张元元等, 2010	
*贺根山Hegenshan(H)	堆晶岩	全岩Sm-Nd	403 ± 27	包志伟等, 1994	
	玄武岩	全岩Ar-Ar	292.85 ± 0.63	Miao et al., 2008	Miao et al., 2008
	辉长岩	锆石 U-Pb	293~295	Miao et al., 2007	
*朝根山Chaogenshan(Cg)	辉长岩	锆石 U-Pb	354 ± 7	Jian et al., 2012	王树庆等, 2008; Nozaka et al., 2002; Miao et al., 2008; Jian et al., 2012
<b>原(古)特提斯洋域 (Paleo-Tethyan ophiolites)</b>					
加拿大Thetford(Th)	辉长岩	角闪石Ar-Ar	477 ± 5	Whitehead et al., 1995	
苏格兰Shetland(Sl)	斜长花岗岩	锆石U-Pb	492 ± 3	Spary et al., 1991	
*玉石沟Yushigou(Y)	辉长岩	锆石 U-Pb	550 ± 17	史仁灯等, 2004	史仁灯等, 2004; 侯青叶等, 2005
	基性熔岩	全岩 Rb-Sr	521.48 ± 23.97	肖序常等, 1978	
东草河Dongchaohe(Dc)	辉长岩	锆石 U-Pb	497 ± 7	曾建元等, 2007	曾建元等, 2007
*松树沟Songshugou(Ss)	石榴辉石岩	锆石 U-Pb	501 ± 10	苏犁等, 2004	
	角闪岩	锆石 U-Pb	973 ± 35(?)	Liu et al., 2004	Dong et al., 2008
	石榴角闪岩	锆石 U-Pb	506 ± 7	Sun et al., 2006	
*大道尔吉Dadaerji(Dd)	辉橄岩	全岩 Sm-Nd	441 ± 58		黄增保2012, 硕士论文
<b>中特提斯洋域 (Meso-Tethyan ophiolites)</b>					
希腊Vourinos(Vr)	辉长岩	锆石 U-Pb	168.5 ± 2.4	Liati et al., 2004	
	斜长花岗岩	锆石 U-Pb	172.9 ± 3.1		
希腊Othris(Ot)	与Vourinos和Pindos同期				
希腊Pindos(Pd)	辉长岩	锆石 U-Pb	171.9 ± 3.1		
阿尔巴尼亚Kukes(Kk)					
阿尔巴尼亚Bulquiza(Bq)	基性侵入岩	单矿物Ar-Ar	160~174	Dimo-Lahitte et al., 2001	
阿尔巴尼亚Shebenik(Sh)					
*丁青Dingqing(Di)	辉长岩	锆石 U-Pb	217.8 ± 1.6	强巴扎西等, 2009	刘文斌等, 2002; 韦正权等, 2007
*东巧Dongqiao(D)	辉长岩	锆石 U-Pb	187.8 ± 3.7	夏斌等, 2008	叶培盛等, 2004; Shi et al., 2012
安多Amdo(Ad)	斜长花岗岩	锆石 U-Pb	188.0 ± 2.0	孙立新等, 2011	赖绍聪等, 2003
那曲Naqu(Nq)	辉长岩	锆石 U-Pb	183.7 ± 1	黄启帅等, 2012	和钟铎等, 2006
*纳木错Xainza(Xz)	辉长岩	锆石 U-Pb	178 ± 10	朱志勇2005, 硕士论文	杨日红等, 2003; 叶培盛等, 2004b

续表1

蛇绿岩	定年样品	定年方法	年龄(Ma)	年龄来源	基性岩数据来源
	橄长岩	锆石 U-Pb	132 ± 3	鲍佩声等, 2007	
洞错Dong Tso(Dt)	辉长岩	全岩 Sm-Nd	191 ± 22	邱瑞照等, 2004	张玉修2007, 博士学位文
	辉长岩	全岩K-Ar	140~152.3		
拉果错Lagkor Tso(Lt)	斜长花岗岩	锆石 U-Pb	166.6 ± 2.5	张玉修等, 2007	王保弟等, 2007; 张玉修2007, 博士学位文
查尔康错Chaerkang (Ct)	闪长岩	锆石 U-Pb	157.5 ± 2.2		张玉修2007, 博士学位文
班公湖Bangong Lake(Bg)	辉长岩	锆石 U-Pb	167.0 ± 1.4	史仁灯, 2007	Shi et al., 2008
<b>新特提斯洋域 (Neo-Tethyan ophiolites)</b>					
塞浦路斯Troodos(Tr)	拉斑玄武岩	全岩Ar-Ar	90.6 ± 1.2	Osozawa et al., 2012	
阿曼Oman (Om)	奥长花岗岩	锆石 U-Pb	95~96	Warren et al., 2005等	
伊朗Neyriz(Ne)	斜长花岗岩	全岩Ar-Ar	92~93	Babaie et al., 2006	
伊朗Esfandagheh(Es)		与Neyriz 同期		Shahabpour et al., 2005	
土耳其Lycian(Ly)	橄榄岩	单矿物K-Ar	102 ± 4	Thuizat et al., 1981	
土耳其Antalya(An)		与Lycian 同期		Robertson, 2002等	
*朗县Langxian(Lx)	辉绿岩	锆石 U-Pb	191.4 ± 3.7	张万平等, 2011	
	辉长辉绿岩	全岩 Sm-Nd	177 ± 31	周肃等, 2001	
*罗布莎Luobusa (L)	辉绿岩	锆石 U-Pb	162.9 ± 2.8	钟立峰等, 2006	
	纯橄岩	锆石 U-Pb	130.0 ± 2.8	徐向珍2009, 博士学位文	
	铬铁矿	锆石 U-Pb	100~120	Yamamoto et al., 2013	
*泽当Zedong (Zd)	中性岩脉	角闪石Ar-Ar	152~156	McDermid et al., 2002	
	枕状玄武岩	全岩 Sm-Nd	175 ± 20	韦栋梁等, 2006	
*仁布Rembu-Dazhuka(Rd)	石英闪长岩	锆石 U-Pb	126 ± 1.5	Malpas et al., 2003	
*大竹曲Dazhuqu(Dz)	岩浆岩单元	全岩U-Pb	120 ± 10	Gopel et al., 1984	
*白朗Bainang (Bn)	角闪岩	角闪石Ar-Ar	123.3 ± 3.1	Guilmette et al., 2009	
*群让Qunrang-Luqu(QL)	辉长岩	锆石 U-Pb	125.6 ± 0.8	李建峰等, 2009	
*吉定Jiding (Jd)	辉长岩	锆石 U-Pb	128 ± 2	王冉等, 2006	Zhang et al., 2005;
*拉孜Lhasa-Buma(Lb)	角闪岩	角闪石Ar-Ar	127.7 ± 2.3	Guilmette et al., 2009	Hebert et al., 2012
*昂仁Angren(Ar)	辉长岩	全岩 Sm-Nd	~166	周肃, 2002	
桑桑Sangsang(Sa)	辉绿岩	锆石 U-Pb	125.2 ± 3.4	夏斌等, 2008	
萨嘎Saga (Sg)					
仲巴Zhongba (Zb)	辉绿岩	锆石 U-Pb	125.7 ± 0.9	Dai et al., 2012	
*当穷Dangqiong (Da)	辉长岩	锆石 U-Pb	126.7 ± 0.4	Chan et al., 2007	
	辉绿岩	锆石 U-Pb	123.4 ± 0.8		
*休古嘎布Xiugugabu (Xg)	辉长岩	全岩 Sm-Nd	126.2 ± 9.1	徐德明等, 2008	
	辉长岩	锆石 U-Pb	122.3 ± 2.4	韦振权等, 2006	
*普兰Yungbwa (Yb)	拉斑玄武岩脉	角闪石Ar-Ar	152 ± 33	Miller et al., 2003	
	辉绿岩	锆石 U-Pb	120.2 ± 2.3	李建峰等, 2008	
*东波Dongbo(Db)	辉长岩	锆石 U-Pb	128 ± 1.1	熊发挥等, 2011	
<b>其他 (太平洋附近, Pacific ocean ophiolites)</b>					
美国Coast Range(CR)	斜长花岗岩	锆石U-Pb	165.58 ± 0.038	Mattinson et al., 2008	
古巴Mayarí-Baracoa(MB)					
古巴Mayarí-Cristal(MC)	地层学年龄		~65	Iturralde-Vinent et al., 2006	
菲律宾Zambales(Za)	斜长花岗岩等	锆石U-Pb	~45.1	Encarnación et al., 1993	
新喀里多尼亚Tiebaghi(TI)			~20	Cluzel et al., 2012	

备注: \*为中国目前已知的铬铁矿矿化区

附表2 中国显生宙典型造山带蛇绿岩及全球主要含矿蛇绿岩地幔橄榄岩数据来源统计表

蛇绿岩	橄榄岩主量	橄榄岩微量 (包括REE)	橄榄岩铬尖晶石	铬铁矿铬尖晶石	铬铁矿PCE	橄榄岩Re-Os	铬铁矿Re-Os
古亚洲洋域							
S	Zhou et al., 2001; Robinson et al., 2005	Robinson et al., 2005	Zhou et al., 2001; Robinson et al., 2005	Zhou et al., 1998 and 2001		Shi et al., 2012(PR)	
My		李行等, 1987	Yang et al., 2012				
H	Robinson et al., 1999; Miao et al., 2008	包志伟等, 1994; Robinson等, 1999; Miao et al., 2008	Robinson et al., 1999		Zhou et al., 1998		
Cg		包志伟等, 1994					
原(古)特提斯洋域							
Y	Song et al., 2009		周会武等, 1995; Song et al., 2009	周会武等, 1995	Zhou et al., 1998		
Ss	陈志宏2004, 博士论文; 苏犁等, 2005; 刘军峰等, 2008; 李桦等, 2010; 于红2011, 硕士论文		王希斌等, 2005; 李桦等, 2010	刘军峰等, 2004			
Dd	黄增保2012, 硕士论文				Zhou et al., 1998		
中特提斯洋域 (BG)							
Dq	刘文斌等, 2002; 韦正权等, 2007	韦正权等, 2007					
D	叶培盛等, 2004; Shi et al., 2012(GR)		王希斌, 1987; Zhou et al., 1998			Shi et al., 2012(GR)	
Xz	朱志勇2004, 硕士论文; 叶培盛等, 2004'			王希斌, 1987			
Dt							
Lt	张玉修2007, 博士论文						
Ct							
Bg	Shi et al., 2008						
新特提斯洋域(YZ)							
L	Zhou et al., 2005; Robinson et al., 2005; 黄圭成, 2006, 博士论文; Xu et al., 2011	Zhou et al., 2005; Robinson et al., 2005; 黄圭成, 2006, 博士论文; Xu et al., 2011	Zhou et al., 1996; 黄圭成2006, 博士论文; Ruskov et al., 2010; Xu et al., 2011; 周二斌等, 2011	Zhou et al., 1996; 1998; 2005; 黄圭成, 2006, 博士论文			
Zd	Dupuis et al., 2005						
Rd	Xia et al., 2003; Dupuis et al., 2005						
Dz							
Bn	Dupuis et al., 2005; Dubois et al., 2005						
Ql							
Jd	Dupuis et al., 2005		Dupuis et al., 2005				
Lb	Dupuis et al., 2005; Dubois et al., 2005						

续表2

蛇绿岩	橄榄岩主量	橄榄岩微量 (包括REE)	橄榄岩铬尖晶石	铬铁矿铬尖晶石	铬铁矿PGE	橄榄岩Re-Os	铬铁矿Re-Os
Sa	Bedard et al., 2009						铬铁矿Re-Os
Sg	Dai et al., 2011						
Zb	黄圭成, 2006, 博士论文						
Da	黄圭成, 2006, 博士论文						
Xg	黄圭成, 2006, 博士论文; Bezaud et al., 2011			黄圭成, 2006, 博士论文			
Yb	Miller et al., 2003; 黄圭成, 2006, 博士论文; 徐向珍等, 2011			黄圭成, 2006, 博士论文		Liu et al., 2012	
Db	黄圭成, 2006, 博士论文						
全球主要含矿蛇绿岩 (GOP)							
CR	Barnes et al., 2013(蛇纹石化)		Choi et al., 2008	Choi et al., 2008			
MB				Proenza et al., 1999	Gervilla et al., 2005; Frei et al., 2006		Gervilla et al., 2005; Frei et al., 2006
MC	Marchesi et al., 2006		González-Jiménez et al., 2011	Proenza et al., 1999; González-Jiménez et al., 2006; González-Jiménez et al., 2011	Gervilla et al., 2005; Frei et al., 2006		
TI	Ulrich et al., 2010						
Ke		Sharma et al., 1996		Melcher et al., 1997	Melcher et al., 1999		Melcher et al., 1999
Pu	Sharma et al., 1995						
Th	Pagé et al., 2009a			Pagé et al., 2009b	Gauthier et al., 1990		
Sl	O' Driscoll et al., 2012			O' Driscoll et al., 2012	O' Driscoll et al., 2012		
Vr	Roberts, 1992; Barth et al., 2008			Roberts, 1992			
Ot	Barth et al., 2008			Barth et al., 2003	Economou-Eliopoulos, 1996		
Pd	Saccani et al., 2004			Pelletier et al., 2008			
Sh				Kapsiotis et al., 2009 and 2011			
Tr	Buehl et al., 2002 and 2004(G.C.A.)	Kay et al., 1976		Buehl et al., 2002 and 2004(G.C.A.); Merlini et al., 2011	Buehl et al., 2004(CC)	Buehl et al., 2002 and 2004(CC)	Buehl et al., 2004(CC)
Om	Godard et al., 2000; Monnier et al., 2006; Hanghoj et al., 2010			Monnier et al., 2006; Hanghoj et al., 2010	Prichard et al., 1996	Hanghoj et al., 2010	Ahmed et al., 2006
Ne	Rajabzadeh et al., 2013			Rajabzadeh et al., 2013	Jamessary et al., 2012		
Es	Shafaii Moghadam et al., 2011, 2012 and 2013; Peighambari et al., 2011			Shafaii Moghadam et al., 2012 and 2013; Peighambari et al., 2011			
An	Aldanmaz et al., 2009 and 2012; Caran et al., 2010			Aldanmaz et al., 2009; Caran et al., 2010			Aldanmaz et al., 2009
Ly	Aldanmaz et al., 2009 and 2012; Uysal et al., 2012			Aldanmaz et al., 2009; Uysal et al., 2012	Uysal et al., 2009	Uysal et al., 2012; Aldanmaz et al., 2012	Uysal et al., 2009

蛇绿岩体代号请见附表1

附表3 中国显生宙典型造山带蛇绿岩及全球主要含矿蛇绿岩稀土元素平均含量统计表

	La	Ce	Pr	Nd	Sm	Eu	Gd	Tb	Dy	Ho	Er	Tm	Yb	Lu	La/Sm	Sm/Yb	LOI
<i>DbH5</i>	0.7357	1.7517	0.5011	0.4381	0.7590	0.7708	0.8077	1.3028	1.3681	1.3707	1.4940	1.5703	1.6316	1.6811	0.455~3.341	0.218~0.637	0.01~12.32
<i>DbD8</i>	0.1611	0.2461	0.0996	0.0669	0.0459	0.0356	0.0332	0.0431	0.0522	0.0607	0.0749	0.0992	0.1088	0.1235	1.990~4.668	0.280~1.623	0~3.17
<i>YbH22</i>	0.1606	0.2576	0.0958	0.0672	0.0485	0.0456	0.0508	0.0625	0.0714	0.0887	0.1100	0.1360	0.1507	0.1747	0.323~5.17	0.098~1.234	0.04~11.13
<i>YbD18</i>	0.1765	0.4132	0.1095	0.0703	0.0425	0.0289	0.0264	0.0336	0.0308	0.0379	0.0457	0.0693	0.0745	0.0980	1.869~6.463	0.222~1.499	0~7.16
<i>XgH13</i>	0.1001	0.0903	0.0773	0.0617	0.0808	0.0971	0.0914	0.1279	0.1419	0.1630	0.1947	0.2089	0.2507	0.2960	0.215~2.585	0.139~1.036	0.50~7.75
<i>DaH3</i>	0.0983	0.0789	0.0575	0.0415	0.0353	0.0510	0.0395	0.0466	0.0582	0.0713	0.0910	0.0964	0.1197	0.1419	2.070~3.016	0.134~0.854	0~0.38
<i>DaD4</i>	0.1353	0.0938	0.0774	0.0547	0.0358	0.0251	0.0224	0.0243	0.0288	0.0348	0.0426	0.0497	0.0677	0.0855	2.055~4.082	0.100~2.344	0~0.50
<i>ZbH10</i>	0.0760	0.0617	0.0495	0.0390	0.0323	0.0252	0.0275	0.0329	0.0445	0.0601	0.0754	0.0961	0.1211	0.1504	1.414~3.498	0.132~0.591	0~2.91
<i>SgH3</i>	0.2280	0.1728	0.1449	0.1723	0.2477	0.1587	0.2125	0.2160	0.2352	0.2439	0.2500	0.2703	0.3584	0.3604	0.554~1.379	0.457~0.617	0.70~5.40
<i>SaH5</i>	0.2547	0.1341	0.0845	0.0788	0.0751	0.0595	0.0280		0.0441	0.0610	0.0573	0.1351	0.0771	0.1802	1.508~6.894	0.555~1.110	5.60~9.00
<i>SaD1</i>	0.3639	0.2648	0.1812	0.2733	0.3604	0.5357	0.4362	0.5556	0.6784	0.7317	0.8125	0.8108	0.8925	0.9459	1.010	0.404	6.60
<i>LbH9</i>	0.0580	0.0457	0.0636	0.0615	0.1444	0.2467	0.1935	0.4784	0.2492	0.4085		0.3664	0.3780	0.3574	0.160~2.316	0.136~0.758	1.5~14.39
<i>LbD1</i>	0.1354	0.0823	0.0652	0.0672	0.0586	0.0417	0.0419	0.0278	0.0326	0.0366		0.0405	0.0832		2.316	0.503	12.75
<i>JdH3</i>	0.0825	0.0593	0.0604	0.0593	0.0578	0.0595	0.0598	0.0525	0.0787	0.0874		0.1441	0.1670	0.2095	1.041~1.939	0.136~0.655	13.08~13.45
<i>QH9</i>	0.0825	0.0215	0.0895	0.0453	0.0558	0.1295	0.0606	0.3323	0.0665	0.2134		0.1471	0.1749	0.2177	0.382~9.436	0.116~0.654	11.06~14.72
<i>QID1</i>	0.0233	0.0152	0.0181	0.0170	0.0541	0.0179		0.0185	0.0231	0.0244		0.0405	0.0507	0.1757	0.431	1.066	13.18
<i>BnH3</i>	0.0175	0.0107	0.0380	0.0103	0.0158	0.1448	0.0257	0.1327	0.0443	0.1280		0.1306	0.1528	0.1667	2.585	0.076~0.117	13.13~13.6
<i>DzH4</i>	0.0480	0.0154	0.0507	0.0517	0.1098	0.1131	0.1422	0.2569	0.1706	0.2683		0.2703	0.3354	0.2973	0.297~7.109	0.029~0.519	0.10~15.22
<i>RdH6</i>	0.1308	0.0878	0.0504	0.0433	0.0471	0.0585	0.0689	0.0826	0.1004	0.1047	0.0613	0.1444	0.1694	0.1899	0.236~13.440	0.052~0.611	8.17~12.07
<i>RdD1</i>	0.1033	0.0851	0.0319	0.0222	0.0205	0.0179	0.0107	0.0065	0.0080	0.0091	0.0127	0.0216	0.0264	0.0405	5.042	0.777	11.70
<i>ZdH2</i>	0.0466	0.0397	0.0380	0.0480	0.1047	0.1042	0.1443	0.1667	0.2062	0.2409		0.2838	0.3702	0.3716	0.277~5.042	0.282~0.284	1.91~11.70
<i>LH15</i>	0.0627	0.0487	0.0461	0.0292	0.0333	0.0455	0.0441	0.0703	0.0764	0.0896	0.1098	0.1356	0.1483	0.1682	0.350~1.939	0.125~1.013	0.95~7.02
<i>LD28</i>	0.0293	0.0217	0.0157	0.0119	0.0118	0.0125	0.0136	0.0166	0.0184	0.0229	0.0263	0.0306	0.0364	0.0511	0.431~15.530	0.029~1.110	0.58~16.40
<i>BgH6</i>	0.0308	0.0195	0.0187	0.0095	0.0165	0.0218	0.0364	0.0525	0.0717	0.0854	0.0927	0.1306	0.1237	0.1577	0.776~12.280	0.093~0.247	10.02~12.49
<i>LiH1</i>	0.1310	0.1459	0.1630	0.1802	0.1982	0.3036	0.2164	0.1852	0.2347	0.2683	0.2396	0.2432	0.2434	0.2703	0.661	0.814	10.11
<i>LiD4</i>	0.0990	0.0999	0.0906	0.0820	0.0721	0.0595	0.0793	0.0880	0.0770	0.0808	0.0849	0.0946	0.0989	0.1216	0.862~3.231	0.208~0.879	12.28~12.57
<i>DiH1</i>	0.0408	0.0231	0.0181	0.0162	0.0158	0.0060	0.0067	0.0093	0.0095	0.0061	0.0083	0.0135	0.0203	0.0270	2.585	0.777	9.29
<i>DiD5</i>	0.0408	0.0353	0.0214	0.0135	0.0099	0.0060	0.0074	0.0093	0.0066	0.0085	0.0108	0.0135	0.0254	0.0324	3.016~4.955	0.139~0.864	5.42~12.97
<i>CtH1</i>	0.1426	0.1042	0.0580	0.0384	0.0248	0.0476	0.0218	0.0185	0.0217	0.0183	0.0229	0.0270	0.0345	0.0405	5.758	0.718	15.43
<i>CtD6</i>	0.1144	0.0928	0.0516	0.0390	0.0244	0.0179	0.0164	0.0131	0.0105	0.0140	0.0135	0.0243	0.0242	0.0324	3.281~5.464	0.148~5.405	11.27~27.95
<i>XzH9</i>	0.3235	0.2685	0.2053	0.1731	0.1101	0.0708	0.0802	0.0844	0.0588	0.0813	0.0810	0.0931	0.0699	0.1066	1.616~6.463	1.110~4.441	14.48~16.35
<i>DqH3</i>	0.0354	0.0276	0.0242	0.0187	0.0150	0.0238	0.0112	0.0108	0.0100	0.0122	0.0111	0.0153	0.0162	0.0225	1.400~4.093	0.666~1.388	11.56~14.94
<i>DH16</i>	0.4363	0.1689	0.1689	0.1233	0.0752	0.0461	0.0521	0.0498	0.0392	0.0385	0.0396	0.0633	0.0460	0.0566	2.486~30.590	0.185~5.235	9.57~18.36
<i>DD2</i>	0.0735	0.0344	0.0308	0.0262	0.0124	0.0060	0.0117	0.0093	0.0095	0.0091	0.0094	0.0054	0.0101	0.0135	4.847~7.238	0.793~2.221	12.45~12.53
<i>DdsD3</i>	0.3396	0.2404	0.2041	0.1649	0.1014	0.0306	0.0660	0.0682	0.0597	0.0565	0.0590	0.0748	0.0690	0.0757	2.900~4.847	0.888~1.832	
<i>YH4</i>	0.0407	0.0314	0.0216	0.0160	0.0085	0.0071	0.0068	0.0065	0.0094	0.0110	0.0144	0.0240	0.0345	0.0486	4.182~4.928	0.063~0.643	0.07~0.45
<i>YD1</i>	0.0827	0.0673	0.0399	0.0350	0.0162	0.0107	0.0136	0.0083	0.0128	0.0122	0.0152	0.0230	0.0379	0.0554	5.098	0.428	0.16
<i>SsH10</i>	0.1338	0.1043	0.0707	0.0569	0.0318	0.0317	0.0250	0.0204	0.0167	0.0152	0.0169	0.0216	0.0241	0.0338	1.616~5.551	0.444~3.273	0.39~4.53
<i>SsD24</i>	0.1412	0.1223	0.0824	0.0628	0.0435	0.0290	0.0373	0.0350	0.0269	0.0302	0.0281	0.0386	0.0334	0.0434	0.711~4.686	0.222~2.498	0.55~13.38
<i>MyP1</i>	0.3930	0.6197		0.5465	0.2928	0.5952	0.1342	0.7407		0.2439	0.1250		0.1014	0.9459	1.342	2.887	
<i>MyD1</i>	0.2183	0.5239		0.5465		0.5357	0.1342		0.0678		0.1667		0.0609				
<i>SH2</i>	0.0146	0.0113		0.0111	0.0225	0.0595	0.0336		0.0136		0.0208		0.0406	0.1351	0.646	0.555	10.79~15.16
<i>SD3</i>	0.0291	0.0300	0.0362	0.0123	0.0225	0.0595	0.0336		0.0136		0.0278		0.0406	0.1351	1.293	0.555	14.53~20.49
<i>CgD1</i>	0.4964	0.3482	0.4457	0.2858	0.2140	0.2202	0.1711	0.2130	0.1737	0.1707	0.1729	0.1757	0.1684	0.1892	2.320	1.271	
<i>HH7</i>	0.1081	0.0885	0.0964	0.0780	0.1089	0.1029	0.1345	0.1786	0.1413	0.1809	0.1872	0.1988	0.1933	0.2143	0.323~4.136	0.093~2.998	12.02~12.98
<i>HD6</i>	0.1235	0.0903	0.1522	0.1349	0.1149	0.1214	0.1049	0.1273	0.0857	0.0988	0.0774	0.1318	0.0984	0.1441	0.738~3.878	0.370~1.271	14.98~15.50
<i>CRsH11</i>	0.0865	4.5511	0.0778	0.0963	0.1276		0.0939	0.1462	0.1673	0.2017	0.2210	0.2322	0.2241	0.2536	0.283~3.339	0.195~1.521	13.80~17.33
<i>MBD6</i>		0.1101		0.1420	0.1770	0.2014	0.1865	0.1867	0.2065	0.2087	0.2101	0.2137	0.2228	0.2588		0.393~0.864	
<i>MBH9</i>		0.0017		0.0030		0.0048	0.0048	0.0049	0.0074	0.0123	0.0197	0.0320	0.0435	0.0686			

续表3

	La	Ce	Pr	Nd	Sm	Eu	Gd	Tb	Dy	Ho	Er	Tm	Yb	Lu	La/Sm	Sm/Yb	LOI
<i>MCH8</i>	0.0010	0.0016		0.0054	0.0116	0.0100	0.0131	0.0078	0.0093	0.0146	0.0217	0.0291	0.0421	0.0639			
<i>MCD2</i>		0.0014		0.0020	0.0047	0.0033	0.0045	0.0046	0.0047	0.0070	0.0096	0.0142	0.0203	0.0311			
<i>TIH3</i>	0.0326	0.0245	0.0194	0.0176	0.0158	0.0134	0.0183	0.0218	0.0276	0.0340	0.0452	0.0554	0.0674	0.0829	0.110-0.316	0.961-4.089	8.98-10.92
<i>OmH158</i>	0.0062	0.0044	0.0035	0.0037	0.0059	0.0092	0.0111	0.0161	0.0242	0.0336	0.0469	0.0588	0.0777	0.1010	0.042-91.314	0.003-0.774	0.13-11.91
<i>OmD49</i>	0.0068	0.0038	0.0034	0.0034	0.0033	0.0082	0.0053	0.0076	0.0115	0.0169	0.0263	0.0371	0.0519	0.0721	0.421-5.193	0.010-0.240	0-15.46
<i>TrP1</i>	0.0218	0.0225		0.0185	0.0225	0.0387	0.0218		0.0217		0.0313		0.0406		0.969	0.555	
<i>LyH56</i>	0.0533	0.0269	0.0176	0.0119	0.0179	0.0195	0.0325	0.0486	0.0532	0.0632	0.0745	0.0911	0.1020	0.1340	0.069-40.347	0.041-0.400	0.45-15.63
<i>LyD5</i>	0.0058	0.0039	0.0039	0.0024	0.0030	0.0012	0.0014		0.0020	0.0047	0.0051	0.0115	0.0144	0.0253	1.293-3.877	0.139	5.17-16.59
<i>AnH34</i>	0.0424	0.0358	0.0163	0.0109	0.0075	0.0085	0.0129	0.0188	0.0239	0.0313	0.0433	0.0601	0.0752	0.1023	1.125-37.162	0.0215-0.4675	0-14.93
<i>AnD12</i>	0.0234	0.0132	0.0081	0.0066	0.0038	0.0028	0.0033	0.0054	0.0051	0.0076	0.0115	0.0194	0.0268	0.0428	1.594-5.009	0.048-0.214	3.30-11.20
<i>EsH17</i>	0.2864	0.0423	0.0340	0.0238	0.0432	0.0834	0.1206	0.2090	0.1277	0.1409	0.1505	0.2043	0.1768	0.1932	0.430-91.314	0.057-0.774	1.571-10.86
<i>EsD4</i>	0.2620	0.1746					0.0839		0.0180	0.0229	0.0240	0.0743	0.0446	0.0449			
<i>PdH2</i>	0.0364	0.0282	0.0543	0.0702	0.1464	0.2976	0.1930	0.5556	0.2714	0.3354	0.3333	0.6757	0.3550	0.4054	0.162-1.293	0.370-0.416	5.03-7.04
<i>OtH15</i>	0.0620	0.0405	0.0290	0.0224	0.0170	0.0246	0.0244	0.0384	0.0530	0.0679	0.0890	0.1054	0.1282	0.1568	0.808-5.922	0.041-0.540	0-13.75
<i>OtD1</i>	0.0233	0.0197	0.0145	0.0118	0.0113	0.0179	0.0151	0.0185	0.0312	0.0366	0.0542	0.0676	0.0832	0.1081	2.068	0.1354	0.89
<i>VrH5</i>	0.0134	0.0109	0.0080	0.0062	0.0054	0.0143	0.0054	0.0116	0.0103	0.0203	0.0233	0.0351	0.0462	0.0649	2.262-2.908	0.098-0.139	0.28-4.30
<i>ThH8</i>	0.0351	0.0341	0.0214	0.0178	0.0104	0.0077	0.0084	0.0120	0.0163	0.0238	0.0342	0.0459	0.0602	0.0824	3.021-3.803	0.165-0.332	5.77-13.32
<i>KeD2</i>	0.0044	0.0046		0.0024	0.0015									0.0181	1.824-5.817	0.063-0.356	
<i>PUH2</i>	0.0049	0.0064	0.0048	0.0047	0.0068	0.0079	0.0106	0.0247	0.0384	0.0528	0.0681	0.0811	0.0994	0.1216	0.431-1.293	0.064-0.074	0-2.88
<i>ABP126</i>	0.3206	0.3752	0.2714	0.2483	0.2446	0.2569	0.2720	0.2976	0.3231	0.3366	0.3582		0.3932	0.4322	0.037-7.878	0.088-1.535	
<i>FAH21</i>	0.0046	0.0038	0.0058	0.0038	0.0109	0.0069	0.0058	0.0073	0.0097	0.0149	0.0228		0.0457	0.0666	0.374-1.481	0.131-0.194	8.05-23.75
<i>FAD8</i>	0.0055	0.0038	0.0037	0.0029	0.0061	0.0046	0.0028	0.0037	0.0050	0.0072	0.0108		0.0234	0.0389	1.747	0.566	9.60-17.58

备注：

- 除11块美国Coast Range蛇绿岩蛇纹石化方辉橄榄岩（CRsH11），其他首列符号为蛇绿岩体代号+岩性（H-方辉橄榄岩；D-纯橄岩）+样品数（如DbH5代表东波蛇绿岩体地幔方辉橄榄岩五个样品，蛇绿岩体代号见附表1）。深海橄榄岩数据（ABP126）来源于Niu(2004)，弧前橄榄岩数据（弧前方辉橄榄岩FAH21和弧前纯橄岩FAD8）来源于Parkinson and Pearce(1998)。其他具体数据来源请见附表2。
- 烧失量（LOI）若出现负值，以0为底限。图中REE平均值、La/Sm、Sm/Yb数值均已将原文给出数据根据原始地幔值（Sun and McDonough, 1989）标准化。文中低检出检测线或未给出具体数值的不在平均值或变化范围内。